Total reaction cross sections for charged particles in the energy range up to 100 MeV

O. F. Nemets, L. I. Slyusarenko, and V. V. Tokarevskiĭ

Institute of Nuclear Research, Academy of Sciences of the Ukrainian SSR, Kiev

Fiz. Elem. Chastits At. Yadra 6, 827–891 (October–December 1975)

The experimental data are systematized for the total reaction cross sections induced by protons, deuterons, ^{3}He nuclei, and α particles in the energy range up to 100 MeV. The methods of measuring the total cross sections are described. The behavior of the total reaction cross sections as functions of the initial energy of the particles and the atomic weight of the target nucleus is discussed. Isotopic effects are analyzed and their relation to the distribution of nuclear density discussed. The theoretical models used to calculate the total reaction cross sections are discussed.

PACS numbers: 25.40.—h

INTRODUCTION

The total cross sections for reactions induced by charged particles with energy less than 100 MeV are among the least studied nuclear constants. In collision theory, one usually considers the total interaction cross section

$$\sigma_t = \sigma_{el} + \sigma_R, \tag{1}$$

which is the sum of the integrated elastic scattering cross section σ_{el} and the total reaction cross section σ_R. The simplest method of calculating the total interaction cross section is based on the optical theorem[1]:

$$\sigma_t = \frac{4\pi}{k} \operatorname{Im} f\ (\theta = 0°), \tag{2}$$

where $f(\theta = 0°)$ is the amplitude of elastic scattering at $\theta = 0°$; k is the wave number of the relative motion. Subtracting the integrated elastic scattering cross section from the total interaction cross section calculated in accordance with Eq. (2), we obtain the required total reaction cross section. This procedure is suitable only for determining the total reaction cross sections induced by neutrons. For charged particles, the elastic scattering amplitude $f(\theta)$ has a singularity at $\theta = 0°$, and the total reaction cross section $\sigma_R = \sigma_t - \sigma_{el}$ is the difference of infinitely large quantities. There exists a generalization of the optical theorem for the case of charged particles proposed by Holdeman and Thaler,[2] and this enables one to avoid the difficulty by taking into account the screening of the Coulomb field. However, the practical application of the modified optical theorem to the calculation of total reaction cross sections from small-angle elastic scattering data for charged particles is restricted to collisions in which only a few partial waves participate.

The total reaction cross section can also be calculated if the absorption cross section σ_a is known:

$$\sigma_R = \sigma_a - \sigma_{CE}, \tag{3}$$

where σ_{CE} is the integrated cross section of elastic scattering accompanied by the formation of a compound nucleus. At energies of the charged particles greater than 10 MeV, $\sigma_{CE} \ll \sigma_{el}$, especially for the scattering of composite particles, and one can therefore assume that $\sigma_R \approx \sigma_a$. In turn, it is convenient to represent the absorption cross section in terms of the collision S matrix. In particular, for spinless particles

$$\sigma_a = \frac{\pi}{k^2} \sum_{L=0}^{\infty} (2L+1)(1 - |S_L|^2), \tag{4}$$

where S_L is a diagonal element of the S matrix. The elements of the S matrix can be determined by phase-shift analysis or they can be calculated theoretically on the basis of one of the models of nuclear reactions (for example, the optical, diffraction, or quasiclassical approximation, etc.).

Concluding our brief discussion of the methods of theoretical analysis of the total reaction cross section, let us mention the connection between the absorption cross section and the imaginary part W of the optical potential[1]:

$$\sigma_a = -\frac{2\mu}{\hbar^2 k} \langle \Psi | W | \Psi \rangle, \tag{5}$$

where Ψ is the solution of the Schrödinger equation with optical potential $U = V + iW$ which satisfies the boundary condition of elastic scattering. The experiment fact that the absorption cross section is nonzero means that there is an imaginary term in the phenomenological interaction potential.

Thus, from the theoretical point of view, to determine the total reaction cross section it is sufficient to parametrize the elastic scattering amplitude. However, the currently used methods of parametrization (phase-shift analysis, optical model, parametrized phase-shift analysis) have a common shortcoming: They are all nonunique to a greater or lesser extent. Therefore, the total reaction cross sections calculated on the basis of elastic scattering data exhibit a very wide spread of values (up to 30–40%). This accuracy is clearly unsatisfactory, and it is therefore necessary to determine the total reaction cross sections experimentally.

Experimental investigations were initiated in 1959 by Gooding[3] and Burge,[4] who proposed two methods for measuring the total cross sections, and also obtained the first experimental results. Between 1959 and 1973, the number of experimental investigations increased to 36, 26 of these being devoted to measurements of proton total cross sections, five to deuteron total cross

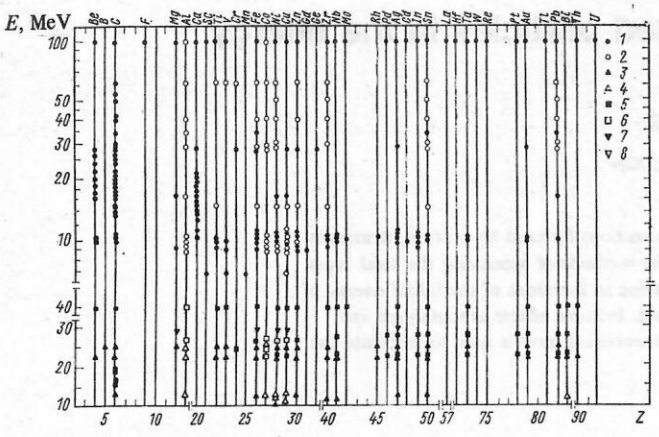

FIG. 1. Extent to which the total cross sections of reactions induced by p, d, ^{3}He, ^{4}He have been studied: 1) and 2) experimental data for protons; 3) and 4) for deuterons; 5) and 6) for α particles; 7) and 8) for ^{3}He; 1), 3), 5), and 7) indicate that the measurements were made on targets with natural isotopic composition; 2), 4), 6), and 8), with single-isotope targets. The energy scale for the protons is logarithmic; for d, ^{3}He, and ^{4}He, it is linear.

sections, and four to α-particle total reaction cross sections; one measurement was made of the total cross section of reactions induced by ^{3}He ions. Figure 1 gives an idea of the extent to which the nuclei of the periodic system have been studied; it gives the elements for which the total cross sections have been studied in the energy range up to about 100 MeV with p, d, ^{3}He, and ^{4}He as initial particles. It can be seen from Fig. 1 that only the proton total reaction cross sections have been studied in any detail.

It is a fairly complicated experimental problem to measure total reaction cross sections. One can therefore very reasonably ask: What new information can be obtained by this experimental effort?

It is a fairly widely held opinion that measurements of total reaction cross sections are necessary because of the requirements of the optical model of the nucleus. The point is that the differential elastic scattering cross sections, the differential polarization cross sections, and the total reaction cross sections are the three main physical quantities calculated in the optical model. Without discounting the importance of the experimental total cross sections for the solution of this complicated problem, we should point out a different informative possibility of this constant which has long been used in high energy physics but has not yet found application in intermediate-energy physics. We are referring to the use of total reaction cross sections to obtain information about the density distribution of nuclear matter and, primarily, parameters such as the radius of the nucleus and the thickness of the boundary layer. If these data are then compared with the results of analysis of the elastic scattering of fast electrons, one can obtain information about the density distribution of neutrons in the nucleus. Similar information can be obtained from the radial dependence of the phenomenological optical potential if one can succeed in reducing the ambiguity that results from analyzing the experimental data in the framework of the optical model. To solve the problem, it is necessary to make measurements on single-isotope targets with an error not greater than 3–5%.

1. METHODS OF MEASURING TOTAL REACTION CROSS SECTIONS

There are three known ways of measuring total reaction cross sections: 1) the method of summation, 2) the method of recoil nuclei, and 3) the attenuation method.

The summation method starts directly from the definition

$$\sigma_R = \sum_b \sigma(a, b), \tag{6}$$

where the summation is over all open reaction channels $A(a,b)B$. The integrated cross sections $\sigma(a,b)$ can be obtained by integrating the differential cross sections, or they can be determined by the method of induced radioactivity. This method is best used when there are few open channels. At higher energies, there are more open reaction channels, which makes the measurements difficult. As a rule, the accuracy with which the cross sections can be measured by this method is not better than 10%.

The *method of recoil nuclei* exploits the obvious fact that in every collision (scattering or nuclear reaction) recoil nuclei are formed. By measuring the total number of recoil nuclei and calculating the fraction corresponding to elastic collisions, we obtain the direct number of all inelastic collisions that determine the sum (6). The method is convenient in the cases when the investigated nuclei are the working medium of the detector. Burge[4] used it to determine the total cross sections of reactions induced by protons in the carbon of a plastic scintillator. The measured energy spectrum is asymmetric, and the low-energy part cannot be separated out without additional investigations. It is first necessary to estimate the contributions of three processes: 1) elastic scattering of the protons on the carbon; 2) the elastic scattering of the protons on protons; 3) the inelastic scattering of protons on the carbon. Analysis of the theoretical and experimental spectra yields the low-energy "tail" from which the absorption cross section is estimated. The error in the determination of the total reaction cross sections is about 10%.

The method can be used with any scintillator, in particular gas and liquid scintillators containing inert gases. It has been shown that inert gases have a greater light output and shorter decay time in the liquid state.[5] The method proposed by Burge can also be applied to solid materials like germanium and silicon if semiconducting radiation detectors are used, but the large errors have prevented its experimental implementation in these cases.

The *attenuation method* consists of determining the relative attenuation of the beam particles as a result of interaction with the target nuclei. If the intensity of the particles in the incident beam is I_0 and that of the attenuated beam is I, then

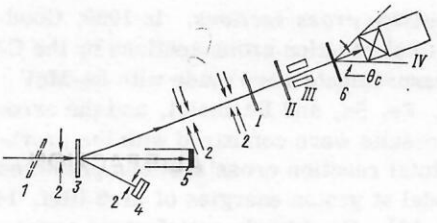

FIG. 2. Arrangement of experiment for measuring total reaction cross sections by the attenuation method using the coincidence–anticoincidence technique: 1) "false" target; 2) collimating slits; 3) target for obtaining the scattered beam; 4) monitor; 5) Faraday cup; 6) investigated target; I–IV are detectors.

$$I = I_0 \exp(-n\sigma_R x), \tag{7}$$

where n is the number of nuclei per cm^3 of the material in the target; x is the thickness of the target; and σ_R is the total reaction cross section.

The value of $n\sigma_R x$ for charged particles does not exceed 10^{-3}, and therefore

$$n\sigma_R x = (I_0 - I)/I_0. \tag{8}$$

In the early investigations of Greenlees and Jarvis,[6] the intensities I_0 and I were measured separately, which led to large errors in the determination of the total cross section. At the present time, there exist two ways of measuring simultaneously the attenuation $\Delta I = I_0 - I$ and the initial intensity I_0: the coincidence–anticoincidence method[3,7,8] (which we shall call the CA method) and the charge integration method[9,10] using Faraday cups (the FC method).

The CA *method.* In the simplest form of the attenuation method with coincidences and anticoincidences, one uses four particle detectors I–IV arranged along the axis of the collimated beam of particles (Fig. 2). The target is placed between III and IV. The signals from the detectors are transmitted to a coincidence–anticoincidence circuit, which records complicated events of the type $12\bar{3}4$ and $12\bar{3}\bar{4}$ (in the notation of formal logic). The number of $12\bar{3}\bar{4}$ events is proportional to the attenuation of the beam due to collisions with target nuclei. The essence of the measurements is to determine $I_0 - I$ and I_0 with the target and $i_0 - i$ and i_0 without the target. Then the total reaction cross section is determined from

$$\frac{I_0 - I}{I_0} - \frac{i_0 - i}{i_0} = n\sigma_R x. \tag{9}$$

It is necessary to take into account nuclear reactions in the detector IV, their cross sections depending on the energy. The energies of the particles in the measurements with and without the target are different for this detector. To eliminate this effect, a "false target" is placed in front of the detector I in the measurements without target; its thickness must be such that the energy of the particles in detector IV corresponds to the energy in the measurements with target. The total reaction cross section with allowance for all the corrections can be represented in the form

$$\sigma_R = \frac{I_0 - I}{nxI_0} - \frac{i_0 - i}{nxi_0} - 2\pi \int_{\theta_c}^{\pi} \sigma_{el}(\theta) \sin\theta\, d\theta + \eta \frac{n'x'}{nx} + 2\pi \int_0^{\theta_c} \sigma_{pq}(\theta) \sin\theta\, d\theta; \tag{10}$$

here, the first term is the beam attenuation in the measurement with target; the second is the background, the beam attenuation in the measurements without target; the third, the correction for elastic scattering; the fourth, the correction for the reactions in the second transmission detector; the fifth, the correction for the emission of charged particles into the solid angle of the fourth detector.

Dicello, Igo, and Roush[8] used a slightly modified form of the CA method to measure the total reaction cross sections at proton energy 14.5 MeV. The last stopping detector was divided into two parts in accordance with its two main functions: 1) of detecting the beam transmitted through the target and 2) detecting inelastic processes with the emission of particles within the angle θ_c (the solid angle of the detector).

This method made it possible to take into account automatically the correction for inelastic processes and eliminate the correction for them in the second transmission detector since it was not necessary to use a false absorber. The expression (10) can be rewritten as

$$\sigma_R = \left(\frac{I_0 - I}{nxI_0} - \frac{i_0 - i}{nxi_0}\right) - 2\pi \int_{\theta_c}^{\pi} \sigma_{el}(\theta) \sin\theta\, d\theta. \tag{11}$$

The electronics used in the experiment was fairly complicated; it is described in Ref. 8.

The experimental difficulties of the CA method are as follows: 1) the heavy load on the electronics (approximately 10^5 pulses/sec); 2) the need to obtain stable beams with intensity 10^5–10^6 pulses/sec; 3) the complexity of allowing correctly for random coincidences. The method is described in detail in Refs. 3, 7, and 8. The error of the measurements is 3–5%.

The FC *method.* In the charge integration method (Fig. 3) the target is placed inside a metallic cup, with which it is in electrical contact. The charge of the cup Δq is increased by Ze whenever collisions take place between the incident particle and the target nuclei that are not accompanied by the emission of secondary charged particles through the entry or exit openings of the target cup (Ze is the charge of the incident particle). Thus, the charge Δq is proportional to the attenuation ΔI of the beam after subtraction of the charged particles

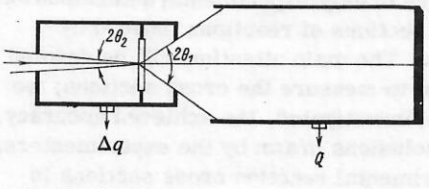

FIG. 3. Arrangement of experiment to measure total reaction cross sections by the attenuation method using two Faraday cups.

that leave the cup. The charge Q of the Faraday cup is proportional to the intensity of the incident beam.

The total reaction cross section is related to the measured charges Δq and Q by

$$\sigma_R = \frac{1}{nx}\frac{(\Delta q - q_b)}{Q} - 2\pi\int_{\theta_1}^{\pi-\theta_2}\sigma_{el}(\theta)\sin\theta\,d\theta + 2\pi\sum_q\left(\int_0^{\theta_1} + \int_{\pi-\theta_2}^{\pi}\right)K\sigma_{pq}(\theta)\sin\theta\,d\theta, \quad (12)$$

where $\sigma_{el}(\theta)$ is the differential cross section of elastic scattering through the angle θ; $\sigma_{pq}(\theta)$ is the differential cross section for the emission of charged particles with charge q at the angle θ integrated over the energy; θ_1 and θ_2 are half the angles subtended by the exit and entry openings of the Δq cup at the center of the target; $K = q/p$ (p and q are the charges of the incident particle and the product particle that leaves the target chamber, respectively); q_b is the charge due to the background components. In order to make both corrections minimal, the angles θ_1 and θ_2 must be chosen on the basis of a compromise.

The charge integration method is suitable for measuring reaction cross sections in nuclei of elements having a good conductivity. If the method is to be implemented in practice, it is necessary to make the background charge q_b minimal, and this entails the solution of the following experimental problems: 1) preparation of beams free of low-energy and neutral particles and also admixtures of other charged particles; 2) prevention of the occurrence of free charges in the Δq cup due to ionization of the residual gas; 3) prevention of the Faraday cups being charged by the γ background; 4) the retention of secondary electrons and β particles from radioactive decay in the target cup; 5) allowance for charge-exchange of particles in the material of the target; and 6) allowance for recoil nuclei that leave the target chamber through the exit opening. The smallest error currently achieved in measurements of the total cross sections by this method is 3–5%. The method is discussed in detail in Refs. 9, 11, and 13.

When experiments are set up in a cyclotron, the CA method suffers from all the difficulties connected with the pulsation of the beam and, above all, the need to allow correctly for random coincidences. Their number depends on the duty cycle of the beam, which may vary from exposure to exposure. In the FC method, the natural modulation of the cyclotron beam is not of great importance, so that this method has definite advantages.

2. REVIEW OF EXPERIMENTS

We consider here briefly experimental determinations of the total cross sections of reactions induced by charged particles. The main attention will be devoted to the method used to measure the cross sections; we indicate the nuclei investigated, the achieved accuracy, and also brief conclusions drawn by the experimenters. A list of the experimental reaction cross sections is given in the Appendix, and graphical material will be given below when we discuss the general behavior of the total reaction cross sections.

Proton total reaction cross sections. In 1959, Gooding[3] investigated total reaction cross sections by the CA method. The measurements were made with 34-MeV protons on C, Al, Fe, Sn, and Pb nuclei, and the error was 5–7%. The results were compared with the previously calculated total reaction cross sections predicted by the optical model at proton energies of 31.5 (Ref. 14) and 40 MeV (Ref. 15). Completely satisfactory agreement was obtained.

In the same year, Burge[4] measured the total reaction cross sections in carbon in the energy range 10–68 MeV with an error of 11–14%. Burge's method is based on a measurement of the low-energy "tail" of the spectrum in the scintillator when it is bombarded by monoenergetic protons. The results were compared with theoretical reaction cross sections calculated earlier in Refs. 14 and 15.

Meyer, Eisberg, and Carlson[16] investigated the total reaction cross sections by the CA method with 60-Mev protons on C, Al, Fe, Sn, Pb nuclei; the error was 6–7%. The experimental data were compared with Gooding's[3] and with the neutron total cross sections at 55 MeV.[17] Satisfactory agreement between all three series of experimental data was obtained. On heavy nuclei, the proton cross sections differ from the neutron cross sections because of the influence of the Coulomb field of the nucleus. Comparison of the experimental data with cross sections calculated by the optical model[14,15] indicates a satisfactory agreement between experiment and the theoretically predicted cross sections.

Investigation of the total reaction cross sections on targets of separated isotopes was begun in 1960 by Meyer and Hintz,[18] who measured the reaction cross sections on monoisotopic targets of C, Al, Co, ^{63,65}Cu, ^{66}Zn and also on Ti, V, Fe, Ni, Ag, Sn targets of natural isotopic composition with 9.85-MeV protons by the method of summation of the integrated cross sections with emission of charged particles and neutrons. The error of the data was 13–16%, and they were compared with the theoretical cross sections obtained by analyzing elastic scattering and polarization at proton energies of 9.8 (Ref. 19) and 10 MeV (Ref. 20).

Albert and Hansen[21] investigated the total reaction cross sections on Cu isotopes with 10-MeV protons; the error was 7% and they used the method of summation of the partial-wave reaction cross sections. They pointed out the good agreement between their experimental data and the theoretical cross sections calculated by Bjorklund and Fernbach[22] with the potential obtained from the best description of elastic scattering and polarization data in the framework of the optical model.

Greenlees and Jarvis[6] measured the total reaction cross sections on natural Cu with 9.3-MeV protons and error 7.5% by the CA method. The experimental results agree well with the data of Refs. 18 and 21 and also with the theoretical cross sections calculated by Easlea[23] using the optical model and a potential with surface absorption ($E_p = 10$ MeV) and also a potential taking into account surface and volume absorption. The theoretical total reaction cross sections found with a

potential allowing for only volume absorption do not agree with the experimental cross sections.

An investigation of the total reaction cross sections on Cu with 9-MeV protons was made by Carlson *et al.*[24] The measurements were made by the CA method. The error of the experimental data was about 9% and they were compared with calculations by the optical model. Carlson *et al.* concluded that the best agreement with the experiments is achieved when one uses either a potential with surface absorption or a potential with volume absorption but with the range of the imaginary part of the potential greater than the range of the real part.

Igo and Wilkins[7] in 1963 were the first to make systematic investigations of the total reaction cross sections on a large number of nuclei. The measurements were made with 10-MeV protons on Be, C, Al, Ti, V, Fe, Ni, Cu, Zn, Zr, Nb, Mo, Ag, Sn, Ta, Au, Pb, and Th nuclei by an improved CA method. The accuracy was about 5–6%, except for the heavy nuclei, for which the error increased to 8–10%. They found that the total reaction cross sections on C and Ni were smaller than on the neighboring nuclei. The experimental data were compared with theoretical data calculated at nearly equal proton energies by the optical model. Potentials with volume and surface absorption gave results that agreed about equally well with the experimental values, and it was difficult to choose a form factor on the basis of the analysis of the total reaction cross sections.

Total reaction cross sections with protons of about 30 MeV were measured by Makino *et al.*[25] on C, Al, Ni, Ag, and Au nuclei with an error of 5% (E_p = 29 MeV), and also by Ridley and Turner[26] on ^{40}Ca, ^{56}Fe, ^{59}Co, ^{58,60}Ni, ^{120}Sn, and ^{208}Pb nuclei with error 4–5% (E_p = 28.5 MeV). The CA method was used. The theoretical reaction cross sections were calculated at the similar energy E_p = 31.5 MeV with a potential allowing for volume absorption, the ranges of the real and the imaginary parts of the potential being taken equal.[14] To within the error of the experiment, the data of Refs. 25 and 16 agree well with the theoretical cross sections of Ref. 14.

The total reaction cross sections at low proton energies (6.75, 8.8, and 9.1 MeV), at which elastic scattering through a compound nucleus is important, were investigated by Dell *et al.*[27] and Bulman *et al.*[28,29] With 6.75-MeV protons, the total reaction cross sections were determined by the method of summation of the partial-wave reaction cross sections on ^{45}Sc, ^{51}V, Mn, and ^{63,65}Cu nuclei with error 7–8%. A comparison with the optical model was made. For the analysis, Perey's parameters[30] extrapolated to 6.75 MeV were used. It was found that the experimental cross sections varied with the mass number faster than predicted by the optical model. With 8.8-MeV protons the reaction cross sections were measured on Al, V, Fe, Co, ^{58,60}Ni, Cu, ^{63,65}Cu, Zn, and Ga nuclei by the CA method with error 5–7%.[28] Perey's parameters were also used to calculate the theoretical reaction cross sections on Al, Ni, Cu, and Zn nuclei. With allowance for the contribution of the elastic scattering through a compound nucleus, it was possible to obtain good agreement with the experimental data except for Co, for which the experimental cross section was greater than the theoretical. Later, Bulman and Griffith[29] measured the reaction cross sections on Mg, Ti, Cu, ^{63,65}Cu, and Zr nuclei with 9.1-MeV protons by the CA method with an error of 4%. The theoretical reaction cross sections were calculated by the optical model with Perey's geometrical parameters[30] and with allowance for the spin–orbit term. Satisfactory agreement was obtained for nuclei of medium atomic weight, $40 < A < 80$.

Pollock and Schrank[31] measured the total reaction cross sections on C, Mg, Al, Ni, Cu, and Pb nuclei with 16.4-MeV protons and error 7% using the CA method. A comparison with the optical model was not made.

Makino *et al.*[32] continued the investigation of the total reaction cross sections with 28-MeV protons and investigated the influence of the closed $1f_{7/2}$ proton shell on the reaction cross sections. The measurements were made by the CA method with error 4% on Cr, Fe, Co, Ni, Cu, Zn, and Ge nuclei. They found that the anomaly in the behavior of the reaction cross sections near Z = 28 MeV includes not only a decrease of the cross section on Ni but also an increase in the cross section on Co. The experimental data were compared with the theoretical cross sections given in Ref. 14. The potential of the optical model used in Ref. 14 allowed for volume absorption (E_p = 31.5 MeV). The agreement with the experiment was not satisfactory.

A systematic investigation of isotope and shell effects was made by Dicello, Igo, and Roush[8] in 1966–1967 with 14.5-MeV protons. The method of Igo and Wilkins in Ref. 7 was significantly improved. Total reaction cross sections were measured on the isotopes ^{49}Ti, ^{54,56,57,58}Fe, ^{58,60,62}Ni, ^{63,65}Cu, ^{64,66,68}Zn, ^{90,91,92,94}Zr, and ^{116,117,118,119,120}Sn with error 2%. The experimental cross sections were compared with the theoretical cross sections obtained by analyzing polarization and elastic scattering data. The reaction cross sections obtained by analyzing the polarization differed somewhat from those obtained from elastic scattering. In both cases, the difference between the experimental and theoretical cross sections exceeded the experimental errors. As a whole, the cross sections predicted by the optical model were smaller than the experimental cross sections, except in the case of Sn, for which the experimental value was lower. The experimental cross sections increased with increasing number of neutrons at constant Z faster than predicted by the optical model for the isotopes of Fe, Ni, Zn, and Zr.

Isotope effects in the total proton reaction cross sections were also investigated by Menet *et al.*[33] The total reaction cross sections were measured with 30-MeV protons on ^{12}C, ^{58}Ni, ^{90}Zr, ^{120}Sn, and ^{208}Pb nuclei; with 40-MeV protons on ^{12}C, ^{27}Al, ^{54,56,57,58}Fe, ^{58,60,62,64}Ni, ^{59}Co, ^{68}Zn, ^{90}Zr, ^{120}Sn, and ^{208}Pb nuclei; with 49.5-MeV protons on ^{12}C, ^{58}Ni, ^{90}Zr, ^{120}Sn, and ^{208}Pb nuclei; with 60.8-MeV protons on ^{12}C, ^{27}Al, ^{50}Ti, ^{51}V, ^{52}Cr, ^{54,56,57,58}Fe, ^{58,60,62,64}Ni, ^{59}Co, ^{68}Zn, ^{90,96}Zr, ^{116}Sn, ^{208}Pb nuclei. It was pointed out that the data agree well with reaction cross sections measured at 30 MeV in Refs. 25 and 26, while the 60.8-MeV data differ from the data

given in Ref. 16. A strict dependence of the reaction cross sections on the neutron excess was found for Ni and Fe isotopes. A similar dependence can be observed for isotopes with $N=28$, although it is less well expressed. The model of an absolutely black nucleus was used for analysis, and completely satisfactory agreement with the experiment was obtained. Analysis by the optical model showed that to describe the experimental data well it is necessary to increase the volume part of the optical potential and decrease the surface part when the proton energy is increased. Attention was drawn to the striking dependence of the product of the depth and diffuseness of the imaginary part of the optical potential with surface absorption on the neutron excess $(N-Z)/A$.

A systematic investigation of the energy dependence of the total reaction cross sections was begun by Delaunay *et al.*[34] and Bearpark *et al.*[35] in 1964. The former investigated the energy dependence of the total reaction cross sections on Ni and Cu nuclei in the energy range 9–12 MeV. They used the CA method and the error of the experimental data was 4–5%. These data were compared with theoretical data calculated with the optical-model potential allowing for surface absorption.

The investigation of the energy dependence of the total reaction cross sections was continued by Bearpark *et al.*,[36] who used a new FC method to measure the reaction cross sections. These were measured on Al, Fe, Co, Ni, ^{58,60}Ni, Cu, ^{63,65}Cu, Zn, Ag, Cd, In, and Au nuclei in the energy range 8.5–11.5 MeV with an error of 3.5–4%. They were compared with the optical model only for Cu, for which good agreement was obtained.

Dicello and Igo[37] investigated the energy dependence of the total reaction cross sections on C in the energy range 9.88–19.46 MeV and on Ca in the range 10.3–21.6 MeV. The total cross sections were measured by the CA method with an error of 12–17% on C and an error of 4–5% on Ca. Dicello and Igo pointed out the resonance nature of the dependence of the total reaction cross sections on the energy for C and Ca. A comparison was made between the reaction cross sections and the integrated cross sections for elastic scattering on ^{12}C and ^{40}Ca, and also the integrated cross section for the excitation of the first state of ^{12}C. A preliminary comparison was made with the optical model for ^{40}Ca (unpublished work of Perey was used). The theoretical cross sections agreed well with the experiment.

The behavior of the proton total reaction cross sections on Be in the energy range 16–28 MeV was investigated by Montague *et al.*[38] The reaction cross sections were compared with the predictions of the optical model based on analysis of elastic scattering. The agreement was good. The reaction cross sections were also analyzed by the model of an absolutely black nucleus, which is usually applied to the investigation of reaction cross sections on nuclei of medium and heavy atomic weights. The simple model correctly predicts the observed energy dependence but one requires a larger value of the radial parameter of the nucleus than in the case of heavier nuclei.

Kirkby and Link[10] measured the total reaction cross sections with 100-MeV protons by the FC method on 41 nuclei from Be to U. Targets of natural isotopic composition were used. The experimental cross sections were compared with theoretical ones calculated in the semiclassical approximation.

Deuteron total reaction cross sections. Igo and Wilkins[39] used the CA method to measure the total cross sections of reactions induced by 22.4-MeV deuterons on Be, C, Al, Ti, V, Fe, Ni, Cu, Zn, Zr, Nb, Rh, Ag, Sn, Ta, Au, Pb, Bi, and Th nuclei with an error of 3–5% in the case of nuclei of light and medium atomic weights and 7–9% in the case of heavy nuclei. The reaction cross sections increased in proportion to $A^{2/3}$ up to Cu, but thereafter they were practically constant up to Au. The experimental data were not analyzed by the optical model.

Mayo *et al.*[40] used the CA method to measure the total reaction cross sections for 25.1-MeV deuterons on B, C, Mg, Al, Ti, V, Fe, Ni, Co, Cu, Zn, Zr, Rh, Ag, Sn, Ta, Au, and Pb with error 3–5%. Their data confirmed the tendency to a dependence on A found by Igo and Wilkins, though their cross sections were larger in absolute magnitude except for the light nuclei. The main difference between the two series of experimental data was the minimum in the region of Ni found by Mayo's group but not by Igo and Wilkins. It should also be pointed out that the reaction cross sections for the group of heavy nuclei Ta, Au, and Pb were appreciably larger than the cross section on Sn; this effect was not observed with 22.4-MeV deuterons. The experimental reaction cross sections on Mg, V, Fe, Ni, Co, Cu, Ag, Au, and Pb were compared with theoretical values calculated by the optical model. It follows from the analysis that the experimental total reaction cross sections agree better with the theoretical ones obtained with an optical-model potential allowing for surface absorption.

The differential cross sections for elastic scattering of deuterons with energy 25.9 and 21.6 MeV and the total reaction cross sections at 25.1 MeV were analyzed by the optical model in Ref. 41. A variation of the diffuseness parameter of the imaginary part of the optical potential made it possible to achieve satisfactory agreement with experiment. The analysis made in Ref. 41 indicated that the parameters of the optical potential depend on the nuclear structure. For nuclei neighboring on ^{58}Ni the parameters of the potential were found to fluctuate, this being reflected in the total cross sections.

An investigation of the deuteron total cross sections on targets of separated isotopes was begun by Budzanowski *et al.*,[42] who measured the total reaction cross sections on ^{12}C, ^{58,60}Ni, and ^{209}Bi with 12.8-MeV deuterons by the method of summation of the partial-wave reaction cross sections. The cross sections were determined with an error of 8–15%. The experimental cross sections were compared with theoretical ones obtained with an optical potential allowing for volume absorption. The experimental and theoretical cross sections agreed well for ^{60}Ni and ^{109}Bi.

Bearpark *et al.*[36] measured the total reaction cross sections on ^{58,60}Ni and ^{63,65}Cu isotopes with deuterons of about 11 MeV by the FC method. They were not compared with the optical model.

The total reaction cross sections of Al, Fe, Ni, ^{60,64}Ni, Co, ^{63,65}Cu, Zn, Ag, and Sn were measured with 13.6-MeV deuterons and an error 2.5–5% by the FC method in Ref. 43. It was found that the deuteron total reaction cross sections varied irregularly in the interval $A \approx 56$–65. The experimental data were analyzed by the optical model using unique and optimal sets of parameters obtained by analyzing the differential elastic scattering cross sections.

Total cross sections of reactions induced by ^{3}He *and* ^{4}He *particles.* Igo and Wilkins[44] determined experimentally reaction cross sections on Be, C, Al, Ti, V, Fe, Ni, Cu, Zn, Zr, Nb, Mo, Ag, Sn, Ta, Au, Pb, Bi, and Th nuclei with 40-MeV α particles by the CA method. The reaction cross sections on light and medium nuclei were determined with an error of 2–3% and on heavy nuclei with an error of 4–6%. The reaction cross sections were found to depend linearly on $A^{2/3}$ from Be to Ti, and then a reduction of the cross section by about 18% was observed in the region of Ni. The experimental results were compared with optical-model calculations. Good agreement was observed for nuclei of medium atomic weight, except for the minimum in the region of Ni. For the light nuclei, the experimental cross sections were smaller than the theoretical; for heavy nuclei, it was the other way round.

Budzanowski *et al.*[45] used the CA method to measure the reaction cross sections on Cr, Fe, Ni, Co, Cu, and Zn nuclei with 24.7-MeV α particles with error 2.5–4%. The total reaction cross sections were found to depend linearly on $A^{2/3}$. A reduction of the cross sections in the region of Ni was not observed. The experimental data were compared with theoretical optical-model data. Agreement was obtained to within the errors of the experiment. The analysis revealed an ambiguity in the determination of the parameters of the optical potential.

The investigation of the total reaction cross sections was continued by the Cracow group with 23.2 and 27.8-MeV α particles.[13] Reaction cross sections were obtained for Ni, Co, Cu, Pd, Ag, In, Sn, Ta, Pt, Pb, and Bi nuclei by the FC method with error 3–5%. The effect of electron capture by an α particle in the material of the target was reduced by placing a carbon foil behind the target. A comparison with theory was not made.

The total reaction cross sections for 27.2-MeV α particles were determined for Al, Fe, Ni, ^{60,64}Ni, Co, Cu, ^{63,65}Cu, and Zn nuclei with an error 3–5% in Ref. 43. The FC method was used to measure the cross sections. The experimental data indicated an anomalous behavior of the reaction cross sections in the region of Ni, and also a more rapid increase of the cross sections on isotopes than follows from the $A^{2/3}$ law. The experimental cross sections were compared with theoretical ones calculated by the diffraction and optical models. Satisfactory agreement with the experiment was obtained on the basis of optical potentials with only surface absorption.

The energy dependence of the total cross sections of reactions induced by α particles on C in the range 15.8–20.1 MeV was investigated by Labie *et al.*[46] An analysis was made using the optical model and a potential allowing for the L dependence of the imaginary part. The experimentally observed minimum in the region of 18.5 MeV was described satisfactorily. Attention was drawn to the correlation between the variations of the total and the differential cross sections (at angle 176°) as functions of the energy.

Total cross sections of reactions induced by ^{3}He particles were measured by Balcarcel and Griffith.[47] The reaction cross sections were determined for Mg, Al, Fe, Ni, Cu, and Ag nuclei with 29-MeV ^{3}He particles with error 2–3% by the CA method. The reaction cross sections were found to increase smoothly with increasing atomic weight. The experimental reaction cross sections were compared with theoretical ones calculated by the optical model.[48,49] Satisfactory agreement was obtained only for the Al nucleus.

Baugh[50] made a detailed analysis of the data of Ref. 47, using an optical-model potential with volume absorption. He obtained good agreement with the experiment.

3. DEPENDENCE OF THE TOTAL REACTION CROSS SECTIONS ON THE ENERGY OF THE INCIDENT PARTICLES

The sparseness of the experimental data for total reaction cross sections means that the dependence of σ_R on E can be investigated in any detail only for the interaction of protons with nuclei. For other particles, the dependence can be followed only in a very narrow energy range.

Let us attempt to sketch here the general picture, indicating the main tendencies in the energy dependence of the total reaction cross sections in the energy range up to 100 MeV, beginning with the light (Be) and ending with the heavy (Pb, U) nuclei, and also some of the characteristic features (resonances in the light nuclei, correlation between the total reaction cross sections and other nuclear processes). The total reaction cross section is the sum of the cross sections of all inelastic processes that result in the particle's being taken out of the entrance channel. The number of open reaction channels increases with increasing energy of the incident particles. The total reaction cross section is influenced by the ratio of the initial particle energy to the height of the Coulomb barrier of the nucleus, and also by the thresholds of the various nuclear reactions. Therefore, σ_R at low energies of the particles will depend very strongly on the energy. At low energies, the wavelength of the incident particle is comparable with the nuclear dimensions, and one usually considers the interaction of the particle with the nucleus as a whole, without allowance for its internal structure. At higher energy, the influence of nucleon–nucleon collisions begins to be manifested, and their importance increases

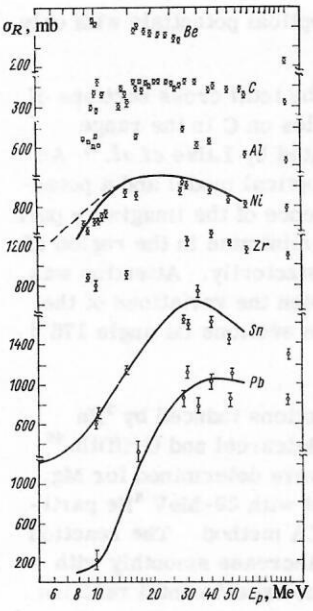

FIG. 4. Energy dependence of experimental proton total reaction cross sections. The continuous curves are the excitation functions calculated in Ref. 51 using unique parameters of the optical potential and with allowance for the cross section of elastic scattering through a compound nucleus; the dashed curve is without allowance for σ_{CE}.

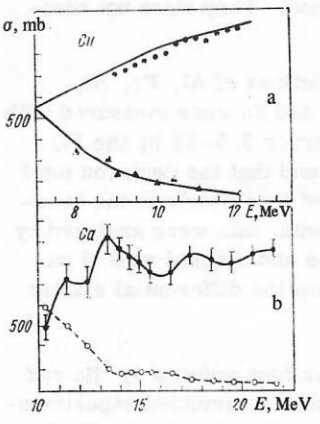

FIG. 6. Comparison of the energy dependence of the proton total reaction cross sections and the integrated cross sections for elastic scattering of protons on Ca and Cu nuclei. a) the black circles are the experimental total reaction cross sections for Cu; the black triangles, the integrated cross section for elastic scattering from 60 to 180°; the continuous curve is a calculation by the optical model of the nucleus. b) The black circles are the total cross sections of reactions on ^{40}Ca; the open circles, the integrated cross sections for elastic scattering from 41 to 180°; the experimental points are joined by curves.

steadily until finally, at high energies, they become predominant.

Let us analyze first the experimentally observed dependence of the total reaction cross sections on the energy of the incident particles (Fig. 4). It should be noted that the experimental data at different energies and for different nuclei were obtained in the majority of cases in different laboratories and sometimes differ considerably at the points of overlap (same energy and the same nucleus). An examination of Fig. 4 shows that the behavior of the reaction cross sections on light nuclei (Be, C, Al) differs from the behavior of σ_R on medium and heavy nuclei (Ni, Zr, Sn, Pb). The reaction cross sections on Be decrease smoothly in the energy range from 10 MeV to 30 MeV, except for the slight structure in the region 15–20 MeV. The best studied nucleus is ^{12}C. In the range 10–17 MeV one observes a clear resonance structure, but then the strength of the resonances is weakened and their frequency reduced, after which σ_R decreases up to 100 MeV.

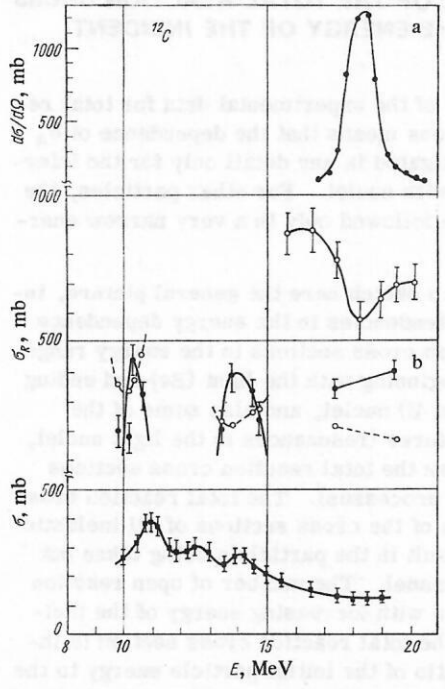

FIG. 5. Energy dependence of total reaction cross sections and the cross sections of elastic and inelastic scattering on ^{12}C: a) the black circles show the differential cross section for elastic scattering of α particles through 176°; the open circles, the total cross sections for α particles. b) The black circles are the proton total reaction cross sections; the open circles the integrated cross sections for elastic scattering of protons from 41 to 180°; the black squares are the integrated cross section for inelastic scattering to the first excited state of ^{12}C ($Q = -4.43$ MeV). The experimental points have been joined by curves for the sake of clarity.

The reaction cross sections for nuclei of medium and heavy atomic weights increase with increasing energy of the incident particles in the region of small E; the energy dependence then exhibits a smooth bend and, finally, a slow decrease right up to 100 MeV. A more detailed analysis of the energy dependence of the reaction cross sections on medium and heavy nuclei is difficult because of the absence of experimental data and also because the measurements were made at intervals of 10 MeV or more.

Let us dwell in slightly more detail on the observed resonance structure in the E dependence of σ_R. This is most clearly expressed for ^{12}C and ^{40}Ca [according to the available experimental data (Figs. 5b and 6b)]. Two peaks are observed in the E dependence of σ_R for ^{12}C: in the region 10.2–10.3 MeV and at 14 MeV. At excitation energies of about 14.6 and 17.1 MeV, which corresponds to this case, a large number of levels of the compound nucleus are excited. The reaction cross section, which is an integral sum of the partial cross sections of the inelastic processes, can have a resonance energy dependence if at least one of the partial excitation functions has such a dependence. Therefore, it need not be attributed to the existence of individual resonance levels of the compound nucleus. In Fig. 5b, we compare the total reaction cross sections and the

integrated cross sections for inelastic scattering on the first excited state of ^{12}C in the proton energy range 10–19 MeV. We observe a correlation between the variations of the total cross sections and the integrated cross sections of inelastic scattering as functions of the energy; this is due to the strong excitation of low-lying states of the ^{12}C nucleus.

At low energies of the incident particles, when processes that proceed through a compound nucleus contribute to the reaction cross section, i.e., when the total reaction cross section can be identified with the cross section for the formation of a compound nucleus, information can be obtained about the density of levels of the compound nucleus on the basis of the experimental data on the total reaction cross sections. With increasing energy of the particles, direct processes become more and more important, and the connection between the density of levels and the total reaction cross section becomes more complicated. The correlation observed in some investigations[43] between the variations of the excitation energy and the total reaction cross section as functions of the atomic weight merely indicates that these two nuclear constants are related to a definite parameter which reflects the structure of the nuclei or the composite systems (particle + nucleus).

Note finally the correlation between the energy dependences of σ_R and the integrated cross section for elastic scattering of protons. With increasing σ_R, the latter decreases (see Fig. 5 and Fig. 6 for ^{12}C, ^{40}Ca, and Cu). A similar picture is observed in the total cross sections of reactions induced by α particles. Figure 5a shows the energy dependence of σ_R and of the differential cross section of elastic scattering at 176° on ^{12}C. One can clearly see the correlation in the energy range 16–20 MeV of the α particles. It is interesting to note that an anomaly is also observed in the proton total cross sections in this energy range; this indicates the importance of the contribution of low-lying states of the ^{12}C nucleus to the total cross section for bombardment by both protons and α particles. In the general case, on the basis of the connection between the total reaction cross section and the total elastic-scattering cross section for charged particles obtained in Ref. 2, we may conclude that the increase in the total elastic-scattering cross section leads to a reduction of the total reaction cross section; this explains the observed effect qualitatively.

We now turn to a comparison of the energy dependence of the experimental total reaction cross sections and the theoretical predictions. The absorption cross section can be written in the form

$$\sigma_R = \pi\lambda\!\!\!^{-2} \sum_{L=0}^{L_{\max}} (2L+1) T_L, \tag{13}$$

where $\lambda\!\!\!^{-} = \hbar/\sqrt{2M(E-V)}$ is the de Broglie wavelength of the relative motion (M is the reduced mass of the particle and the target nucleus; V is the height of the corresponding Coulomb barrier; E is the energy of the incident particle); L is the angular momentum of the relative motion.

The transmission coefficient T_L can be expressed in terms of the S-matrix element by

$$T_L = 1 - |S_L|^2. \tag{14}$$

To calculate T_L, it is necessary to use one of the model representations.

Qualitative conclusions can be drawn from the model of strong absorption, in which it is assumed that

$$T_L = \begin{cases} 1 & \text{for } L \ll L_0; \\ 0 & \text{for } L > L_0, \end{cases} \tag{15}$$

where L_0 is the critical angular momentum corresponding to a grazing collision of the incident particle with the nucleus:

$$L_0 = kR\sqrt{1 - V/E}; \tag{16}$$

$$\left.\begin{aligned} R &= r_0 A^{1/3} + \lambda\!\!\!^{-}, \quad \text{if } \lambda\!\!\!^{-} \ll r_0 A^{1/3}; \\ R &= r_0 A^{1/3} + r_r, \quad \text{if } \lambda\!\!\!^{-} \sim r_0 A^{1/3}; \end{aligned}\right\} \tag{17}$$

here, r_r is the radius of the incident particle. Then

$$\sigma_R = \pi R^2 (1 - V/E). \tag{18}$$

In accordance with (18) and with allowance for (17), the total reaction cross section increases monotonically, reaching its limiting value for $E \gg V$:

$$\sigma_R = \pi R^2. \tag{19}$$

With a further increase of the energy, a dependence of the reaction cross section on the energy occurs in (19) through the dependence of R on $\lambda\!\!\!^{-}$. This expression gives a good approximation of the experimental data for the proton total reaction cross sections for Be in the energy range 15–30 MeV, although Eq. (19) is more valid for nuclei of medium and heavy atomic weights. When Eq. (19) is used to describe the energy dependence of the total reaction cross sections one can obtain unambiguous information about the sizes of the nuclei. However, in order to clarify this possibility, additional investigations are required: In what energy range is this equation valid and for what types of incident particle (see Sec. 4)?

The transmission coefficient of the Coulomb barrier of the nucleus can be determined numerically in the framework of the optical model of the nucleus, which, as is shown in Refs. 33–35 and 38, can be successfully used to describe the energy dependence of the total reaction cross sections. Taking into account the energy dependence of the optical-potential parameters, to calculate T_L it is desirable to use unique (or averaged) sets suitable for explaining the differential cross sections of elastic scattering in a wide energy range. At the present time, unique sets have been obtained for protons in the energy range up to 60 MeV (Refs. 51 and 54) and for deuterons up to about 20 MeV (Ref. 55). For ^4He ions the literature data have not yet been systematized.

In Fig. 4, the continuous curves are the excitation functions for the total reaction cross sections calculated in Ref. 51 using unique parameters found from a global

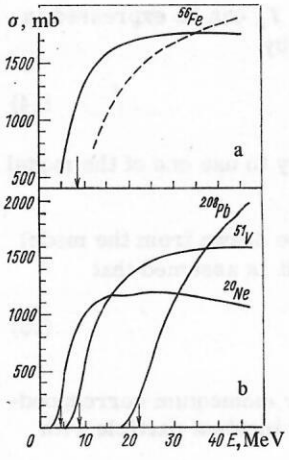

FIG. 7. Energy dependence of the total cross sections of reactions on ^{56}Fe induced by deuterons (a) and on ^{20}Ne, ^{51}V, ^{208}Pb induced by α particles (b). The dashed curve is a calculation in the semiclassical approximation.

search (the values of the parameters are given in Sec. 8). There is a perfectly satisfactory explanation of the observed energy dependence, especially for the Sn and Pb nuclei.

Similar calculations using Perey's potential[55] were made in Ref. 56, in which the energy dependence of the deuteron total reaction cross sections was investigated in the range 5–45 MeV for ^{56}Fe (Fig. 7a). The reaction cross sections increase strongly with increasing energy from 5 to 15 MeV, and one then observes a slower increase of the cross sections up to 30 MeV. Beginning at 30 MeV, the reaction cross sections hardly depend on the energy at all, i.e., the behavior of the cross sections above 30 MeV no longer depends on the Coulomb barrier of the nucleus. For comparison, in Fig. 7a, we show the energy dependence of the total cross section obtained when the expressions (17) and (18) are used to take into account the Coulomb interaction. Equation (18) only qualitatively predicts a dependence of the cross section on the energy and then only up to the "saturation" region.

The total cross sections of reactions induced by α particles on nuclei from Ne to U in the energy range up to 46 MeV (see Fig. 7b) were investigated theoretically by Igo and Huizenga[57] and Igo and Planck.[58] The calculated reaction cross sections were found to increase strongly with increasing energy, exhibiting a dependence similar to the deuteron and proton cross sections considered above.

In the energy range 30–60 MeV an attempt was made to describe the energy dependence of the proton total reaction cross sections by means of the intranuclear cascade model.[59] The energy range 30–60 MeV for protons lies far from the Coulomb barrier, even for heavy nuclei. Although an agreement with experiment to within 10% was achieved, it is necessary to justify the application of this model at such low energies. Earlier, the model had been used to describe the cross sections of reactions induced by protons in the range 350–3500 MeV.

Thus, at the present time it is only by means of the optical model of the nucleus that one can describe the energy dependence of the total reaction cross sections for light to heavy nuclei and for different types of particles. By introducing a dependence on L into the imaginary part of the potential one can describe the behavior of σ_R in the region of the resonances; this was done, for example, for the case of α particles in Ref. 46. In a small energy range one can also describe the energy dependence of the total cross sections of reactions induced by protons by means of the semiclassical expression (19).

4. DEPENDENCE OF THE TOTAL REACTION CROSS SECTIONS ON THE MASS NUMBER OF THE TARGET NUCLEUS

The nature of the functional dependence of the total cross sections of charged particles on the atomic weight of the target nucleus is determined by the ratio of the height of the Coulomb barrier to the initial energy of the particles. The reaction cross sections increase with increasing geometrical size of the nuclei if the reaction cross sections are not affected by the Coulomb field of the nucleus, which is the case at particle energies appreciably higher than the Coulomb barrier of the nucleus. At energies comparable with the height of the Coulomb barrier one observes a competition between the increase in the geometrical cross sections of the nuclei and the reduction of the transmission coefficients due to the increased height of the Coulomb barrier. Similar effects occur in a narrower range of atomic weights in the region of both medium and heavy nuclei. Therefore, it is desirable to consider the dependence of the total cross sections on the atomic weight at particle energies considerably exceeding the height of the Coulomb barrier of the nucleus. On the other hand, with increasing energy the wavelength of the incident particle decreases, and the importance of nucleon–nucleon collisions increases. These two factors must be taken into account when one considers the dependence of the reaction cross sections on the atomic weight of the target nucleus.

The reaction cross sections are shown as functions of the atomic weight for protons of 100 MeV (Ref. 10), deuterons of 25.1 MeV (Ref. 40), α particles of 40 MeV (Ref. 44) and ^{3}He particles of 29 MeV (Ref. 47) in Fig. 8. It can be seen that for all types of particles there is a region in which the total cross sections are proportional to $A^{2/3}$, i.e., proportional to the geometrical cross sections of the nuclei. Thus, the total reaction cross sections at a proton energy of 100 MeV increase linearly with increasing geometrical size of the nuclei in the whole range of atomic weights. Small fluctuations are observed only in the region of Sn and Au–Pb. The total cross sections of reactions induced by deuterons and α particles vary irregularly as a function of the atomic weight of the target nuclei. Characteristic irregularities are observed in the region of Ni, Sn, and Pb, i.e., for nuclei that have closed proton shells with $Z = 28$, 50, 82. The deepest "dip" in the total reaction cross sections is observed on Ni for deuterons and α particles. The anomalous behavior of the total cross sections in the region of Ni will be considered below.

Here we shall merely attempt to establish whether

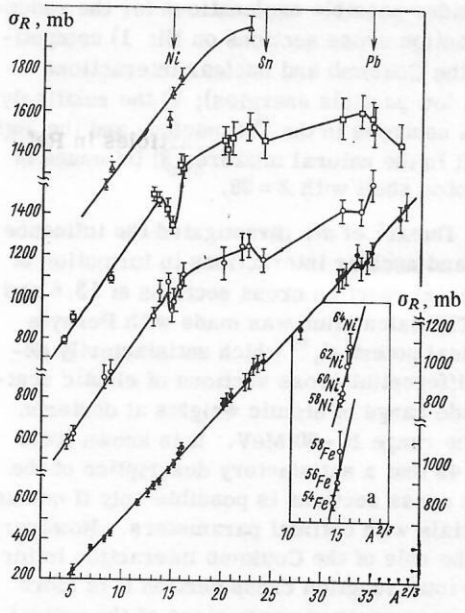

FIG. 8. Total reaction cross sections as functions of the atomic weight of the target. The open triangles are the reaction cross sections for 29-MeV ^{3}He particles[47]; the open squares are the total reaction cross sections for 40-MeV α particles[44]; the open circles are the total reaction cross sections for 25.1-MeV deuterons[40]; the black circles are the total reaction cross sections for protons with an energy of about 99 MeV (Ref. 10) (left-hand scale). a) Dependence of σ_R on $A^{2/3}$ for Fe and Ni isotopes for 60.8-MeV protons[33] (right-hand scale).

the observed irregularities in the behavior of the total reaction cross sections in the region of Ni, Sn, and Pb could be explained by competition between the Coulomb and nuclear interactions. In Ref. 56, Dubar' *et al.* made a theoretical calculation of the reaction cross sections for 13.6 and 22.4-MeV deuterons as a function of the atomic weight using Perey's averaged optical potential[55] (Fig. 9). The two dependences of σ_R on A are effectively coincident only up to $A \approx 20$, after which the discrepancy between them increases with increasing atomic weight of the target nucleus. The curves for the two deuteron energies have different forms. At 13.6 MeV the reaction cross sections increase smoothly up to $A \approx 50$; in the range $50 < A < 100$ the cross sections are practically constant. In the range $100 < A < 160$ one observes irregularities in the behavior of the cross sections. This is the region of the sub-barrier and superbarrier energies (12–15 MeV), where the influence of the Coulomb field of the nucleus is most important. Beginning with $A > 160$, the reaction cross sections decrease smoothly to U. With 22.4-MeV deuterons the reaction cross sections increase with increasing atomic weight of the nuclei up to $A \approx 100$; in the range $100 < A < 180$ one observes irregularities in the behavior of σ_R and, finally, beginning with $A > 180$, the cross sections decrease smoothly. The competition between the Coulomb and nuclear interactions does not explain the experimentally observed reduction of the cross sections in the region of Sn and Pb; it is evidently due solely to the influence of the closed proton shells. As regards Ni, as we have already noted, the deepest dip is observed here in the total reaction cross sections. The competition between the Coulomb and nuclear interactions at these energies of deuterons and α particles can reduce the reaction cross section by not more than 0.3–1.0%. Another possible explanation of the reduction of the cross section on Ni is the relatively low content of neutrons in the ^{58}Ni nucleus and the large proportion of ^{58}Ni in the natural mixture (see below).

At proton energies exceeding the Coulomb barrier of the nuclei, including the case of heavy nuclei, the dependence of the total reaction cross sections on the atomic weight can be well approximated by Eq. (19). Comparison of the experimental and theoretical cross sections enables one to determine the radial parameter r_0 of the nucleus. This is a very important nuclear constant and a unique determination of it could be very helpful. However, the value of r_0 determined in this way does not always reflect physical reality, especially in the cases when the reaction cross sections vary irregularly with the energy. Thus, the parameter r_0 obtained by comparing experimental and theoretical reaction cross sections may be a function of the energy. In the region of 100 MeV the reaction cross sections are reduced by the influence of nucleon–nucleon interactions. The parameter r_0 determined from the reaction cross sections in this energy range may be underestimated, i.e., it may again be a function of the energy. The optimal energy for determining r_0 is the energy at which the influence of the Coulomb field of the nucleus has been reduced but the nucleon–nucleon interactions have not yet become significant.

Figure 8a shows the total cross sections on Fe and Ni isotopes as functions of the atomic weights of the isotopes for 60–8. MeV protons. It can be seen clearly that the reaction cross sections on the isotopes increase faster than follows from the general dependence of cross sections on the atomic weight of the target nuclei (see σ_R at $E_p = 100$ MeV). This question will be considered in Sec. 6.

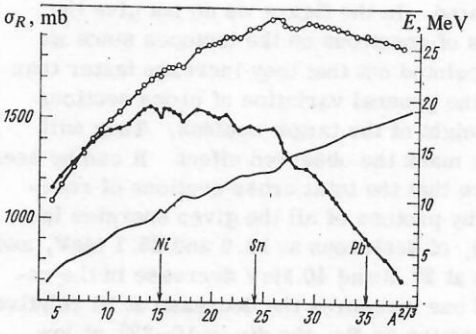

FIG. 9. Deuteron total reaction cross sections as functions of the atomic weight of the target, calculated by the optical potential[56] with Perey's unique set of parameters[55]: the black circles show σ_R^T for 13.6-MeV deuterons; the open circles, σ_R^T for 22.4-MeV deuterons. The curves join the calculated points (left-hand scale); the continuous curve is the height of the Coulomb barrier (right-hand scale).

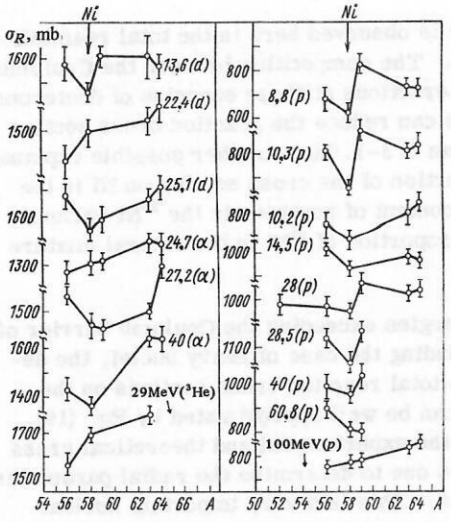

FIG. 10. Behavior of total cross sections for reactions induced by p, d, ^{3}He, and ^{4}He in the region of Ni. The lines join the experimental points; the experimental data are taken from Refs. 7, 8, 10, 26, 28, 32, 33, 36, 39, 43–45, 47.

5. ANOMALOUS BEHAVIOR OF THE REACTION CROSS SECTIONS IN THE REGION OF NICKEL

It is still a matter of dispute whether the reaction cross sections on nickel are lower than on the neighboring nuclei: some experimental data indicate that they are, others do not. The observed reduction of the cross section on nickel is 10–20% of σ_R. This also explains the main difficulty in its determination. At the present time, the error in determination of the total reaction cross section by any method is at least 3–5%. It should be pointed out that this error is the error in measurement of the absolute value of σ_R; the relative dependence of cross sections can be determined with greater accuracy.

Let us consider the experimental data. The dependence of σ_R on A in the region of Ni for protons in the range 8.8–100 MeV, deuterons at 13.6, 22.4, and 25.1 MeV, α particles at 24.7, 27.2, and 40 MeV, and ^{3}He particles at 29 MeV is shown in Fig. 10. In the majority of cases, targets of natural isotopic composition were investigated. In the figure we do not give the cross sections of reactions on the isotopes since we have already pointed out that they increase faster than follows from the general variation of cross sections with atomic weight of the target nucleus. They will therefore only mask the observed effect. It can be seen from the figure that the total cross sections of reactions induced by protons of all the given energies (except 100 MeV), of deuterons at 13.6 and 25.1 MeV, and of α particles at 27.2 and 40 MeV decrease in the region of Ni. If one measures the decrease at Ni relative to the cross section on Fe, the dip is 10–23% at low proton energies and 3–12% at energies appreciably higher than the Coulomb barrier of the nucleus, while it is 9–12% for deuterons and 6–9% for α particles. For 22.4-MeV deuterons, 24.7-MeV α particles, and 29-MeV ^{3}He particles no irregularities are observed in the region of Ni.

Let us consider possible explanations for the reduction of the reaction cross sections on Ni: 1) competition between the Coulomb and nuclear interactions (especially at low particle energies); 2) the relatively low content of neutrons in the ^{58}Ni nucleus and the high content of ^{58}Ni in the natural mixture; 3) influence of the closed proton shell with $Z = 28$.

In Ref. 56, Dubar' *et al.* investigated the influence of the Coulomb and nuclear interactions in formation of the deuteron total reaction cross sections at 13.6 and 22.4 MeV. The calculation was made with Perey's averaged optical potential,[55] which satisfactorily describes the differential cross sections of elastic scattering in a wide range of atomic weights at deuteron energies in the range 10–30 MeV. It is known from Refs. 33 and 43 that a satisfactory description of the total reaction cross sections is possible only if one uses optical potentials with optimal parameters. However, to elucidate the role of the Coulomb interaction in formation of the total reaction cross section it is more convenient to use averaged parameters of the optical potential in order to avoid a possible masking of the "Coulomb effects" by changes in the structure of the neighboring nuclei. It can be seen from Fig. 9 that in the range $56 \leq A \leq 65$ irregularities are observed in the theoretical reaction cross sections. Nevertheless, although the theory predicts a reduction of the cross section on Ni by 2% (0.3%) compared with Fe at deuteron energies of 13.6 MeV (22.4 MeV), the experiment gives 8 (9)%. Thus, although the competition between the Coulomb and the nuclear interactions does become significant in the observed irregularities of the total cross sections at low deuteron energies, it is not the only factor. With increasing deuteron energy, the strength of the Coulomb repulsion decreases and the irregularities in the Fe–Ni–Co region are smoothed in the calculated curves, although the experimental data do not indicate a disappearance of the effect.

The dependence of the total reaction cross sections on the relative neutron excess will be analyzed below. Here we shall only consider the conclusions. The total cross sections of reactions on Fe, Ni, Cu, Zn, and Zr isotopes increase by 5–15% in the transition from the light to the heavier isotopes, i.e., nuclei with relatively low neutron excess $(N-Z)/A$ have smaller cross sections than nuclei with large neutron excess. The dependence of σ_R on $(N-Z)/A$ for nuclei in the region of Ni (deuterons with initial energy 13.6 MeV) is shown in Fig. 11. It can clearly be seen that ^{58}Ni, which has the smallest neutron excess among these nuclei, also has the smallest total cross section. The particular

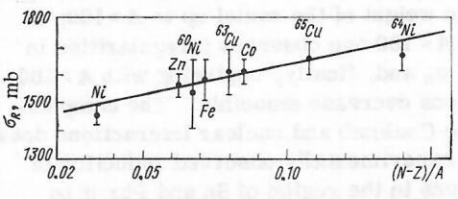

FIG. 11. Experimental total reaction cross sections for 13.6-MeV deuterons as a function of $(N-Z)/A$.

TABLE 1. Values of the parameter r_0 from analysis of the total cross sections of reactions induced by protons, deuterons, and α particles in accordance with the model of an absolutely black nucleus with sharp boundary.

Nucleus	E_p, MeV			E_d=13.6 MeV	E_α=27.2 MeV
	14.5	28.5	99		
^{54}Fe	1.06±0.02	—	—	—	—
^{56}Fe	1.17±0.02	1.35±0.03	—	—	—
^{57}Fe	1.14±0.02	—	—	—	—
^{58}Fe	1.20±0.02	—	—	—	—
Fe	—	—	1.09±0.01	1.28±0.03	1.32±0.02
^{59}Co	—	1.35±0.02	1.10±0.01	1.27±0.02	1.22±0.02
^{58}Ni	1.10±0.02	1.25±0.02	—	—	—
^{60}Ni	1.12±0.02	1.26±0.03	—	1.22±0.05	1.28±0.02
^{62}Ni	1.17±0.02	—	—	—	—
^{61}Ni	—	—	—	1.28±0.02	1.32±0.02
Ni	—	—	1.10±0.01	1.19±0.01	1.23±0.02
^{63}Cu	1.11±0.02	—	—	1.25±0.03	1.21±0.02
^{65}Cu	1.11±0.02	—	—	1.26±0.02	1.25±0.02
Cu	—	—	1.11±0.01	—	—
^{64}Zn	1.09±0.02	—	—	—	—
^{66}Zn	1.13±0.02	—	—	—	—
^{68}Zn	1.14±0.02	—	—	—	—
Zn	—	—	1.13±0.01	1.21±0.02	1.33±0.02

interest in the Ni nucleus is also due to the fact that in the majority of investigations targets of natural isotopic composition were investigated, and Ni, which has a high percentage of the light isotope ^{58}Ni, occupies a distinguished position among the other elements heavier than Ca in that it has the smallest $(N-Z)/A$. Therefore, the connection between the total cross section and the neutron excess is manifested most strongly in the region of Ni.

Finally, let us consider the influence of a closed shell with magic proton number. The absence of experimental data prevents a detailed analysis, though one can note that the observed reduction in the reaction cross sections on the Sn and Pb nuclei with $Z=50$ and 82 indicates that the reduction of the total cross section on Ni is at least partly due to the influence of the closed proton shell with $Z=28$.

6. ISOTOPIC EFFECTS IN THE TOTAL REACTION CROSS SECTIONS

The existence of a proportionality between the total reaction cross sections and the geometrical cross sections of the nuclei gives hope that the total reaction cross sections contain information about the nucleon density distribution in the nucleus. To investigate this possibility, we shall make a calculation of the constant r_0, the radius of the equivalent distribution, for several isotopes, using the model of an absolutely black nucleus with a sharp boundary, on the basis of the experimental proton total cross sections [E_p=14.5 MeV (Ref. 8), E_p =28.5 (Ref. 26), E_p=99 MeV (Ref. 10)], the total deuteron cross sections [E_d=13.6 (Ref. 43)], and the total cross sections of reactions induced by α particles [E_α=27.2 MeV (Ref. 43)]; we use Eq. (19). In order to reduce the influence of the change in the height of the Coulomb barrier of the nucleus on the total cross section, we shall consider only nuclei with nearly the same Z. The values obtained for the parameter r_0 are given in Table 1. The averaged values $\langle r_0 \rangle$ for all nuclei for the three types of particle are fairly close to each other and are equal to 1.13±0.02 (E_p=14.5 MeV); 1.30±0.03 (E_p=28.5 MeV); 1.10±0.01 (E_p=99 MeV); 1.25±0.02 (E_d=13.6 MeV); 12.8±0.02 (E_α=27.2 MeV). For 99-MeV protons, r_0 is appreciably smaller, this being due to the reduction of the proton total cross sections near E_p=100 MeV because of the decrease in the cross section of nucleon–nucleon scattering. For some nuclei, the deviation of r_0 from the averaged value exceeds the experimental errors, which reflects the influence of individual features of the nuclei on the total reaction cross section. The search for the origins of this influence must be begun with an analysis of the dependence of the total reaction cross sections on the neutron number N and the proton number Z, i.e., by comparing the total reaction cross sections on isotopes and isotones. The available experimental data are shown in Figs. 12 and 13. It can be seen from a comparison of these figures that for practically all the investigated isotopes the total reaction cross sections increase systematically with increasing number of neutrons in the nucleus at unchanged Z; if the number of protons is increased at unchanged N, the total cross sections decrease as a rule or remain unchanged to within the experimental errors. We shall refer to the more rapid increase of the total reaction cross sections with increasing number of neutrons in the nucleus as compared with the change of the total cross sections with increasing number of protons in the nucleus as the isotope–isotone effect in the total reaction cross sections. The isotope–isotone effect is manifested for different nuclei, different energies, and different types of incident particles; therefore, despite the still appreciable experimental errors, we may say that we are here dealing with a new phenomenon that characterizes the properties of nuclei.

In the investigation of the elastic scattering of protons, deuterons, and α particles, two new types of

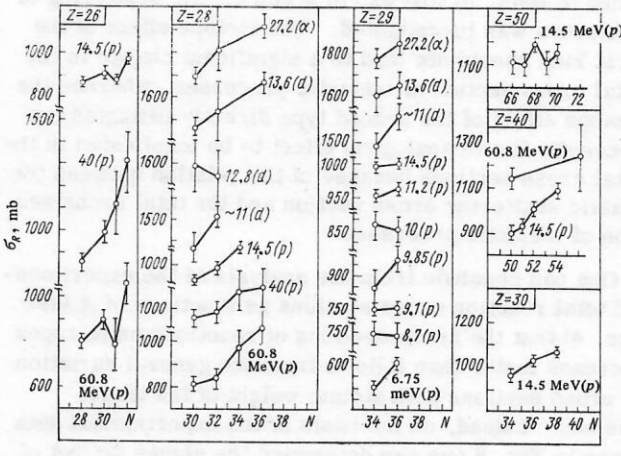

FIG. 12. Total cross sections of reactions on isotopes as functions of the number of neutrons in the nuclei. The lines join the experimental points, and the values of the total reaction cross sections are taken from Refs. 8, 18, 21, 27, 29, 33, 36, 42, and 43.

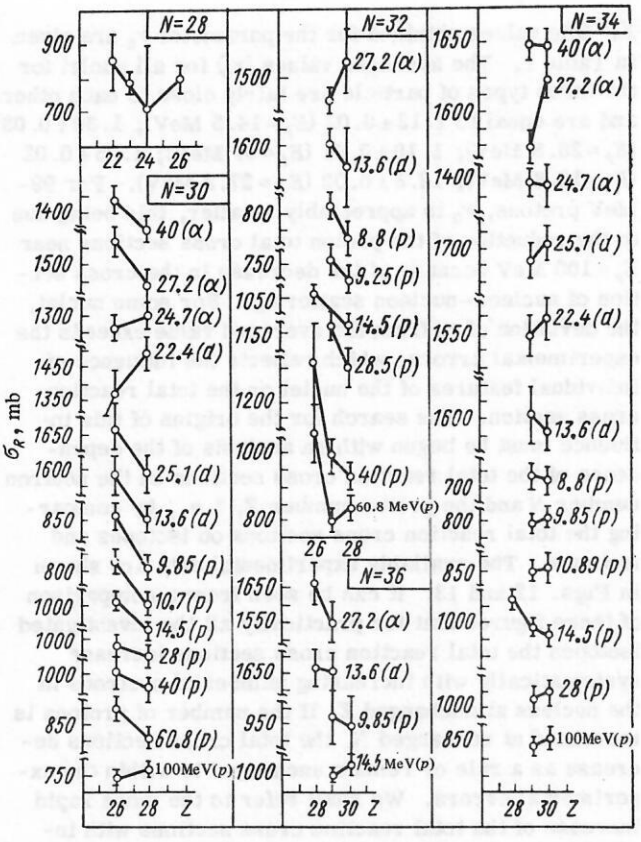

FIG. 13. Total cross sections of reactions on isotones as functions of the number of protons in the nuclei. The lines join the experimental points, and the values of the total reaction cross sections are taken from Refs. 8, 10, 18, 26, 28, 32, 33, 36, 39, 40, 43, and 45.

isotope effect were discovered: 1) a change in the position of the maxima and minima in the angular distribution without a change (or with only a slight one) of the integrated cross section; 2) a change in the profile of the angular distribution (for example, the large-angle effect found in Ref. 60 in proton elastic scattering) or the pronounced change of the integrated cross sections found in Refs. 61 and 62, in which elastic scattering of deuterons was investigated. The isotope effect of the first kind should not lead to a significant change in the total cross section of inelastic processes, whereas the isotope effect of the second type directly indicates the necessity for an analogous effect to be manifested in the total cross sections because of the relation between the elastic scattering cross section and the total cross section of inelastic processes.

One can conclude from the analysis of the experimental total reaction cross sections as functions of A (see Sec. 4) that the cross sections of reactions on isotopes increase faster than follows from the general variation of cross sections with atomic weight of the target nucleus. Indeed, on the basis of the experimental data given in Fig. 8 one can determine the slopes $\Delta\sigma/\Delta A$ of the straight lines, which fit the dependence of the total reaction cross sections on $A^{2/3}$ (for deuterons and α particles, the range of atomic numbers is such that the influence of the Coulomb field of the nucleus has practically no effect). The average slope for 99-MeV protons is 9.6 ± 3.5; for 25.1-MeV deuterons it is 16.9 ± 3.5; for 40-MeV α particles it is 12.1 ± 3.3. Much larger slopes are obtained for the $A^{2/3}$ dependence of the total reaction cross sections on separated isotopes. For the Fe and Ni isotopes with 60.8-MeV protons we have, respectively (for only a nominal "straight line") 65.2 ± 30.5 and 37.0 ± 18.5 (these are cross sections at an energy much higher than the Coulomb barrier of the nuclei). Figure 14 (from Ref. 63) demonstrates the more rapid variation of the total reaction cross sections on isotopes than the one predicted from the $A^{2/3}$ proportionality.

The difference between the behavior of the total reaction cross sections for isotopes and isotones can partly be explained by the influence of the Coulomb field of the nucleus. To confirm this, let us consider the behavior of the theoretical reaction cross sections calculated by the optical model. The advantage of these calculations is the correct allowance for the influence of the Coulomb field of the nucleus on the total reaction cross sections. In Figs. 15a and 15b, we give the total reaction cross sections for Cr, Fe, Ni, and Zn isotopes calculated by the optical model using Perey's[55] unique set B for 13.6-MeV and 22.4-MeV deuterons.[56] As can be seen from Fig. 15, the values of σ_R for the isotopes of this element increase with increasing number of deuterons, forming "isotope" straight lines. For 13.6-MeV deuterons, the "isotope" straight lines for different elements are shifted relative to one another and almost coincide at 22.4 MeV. The slopes of the isotope straight lines in the two cases are very nearly equal, as can be seen by comparing the values of $\Delta\sigma/\Delta N$, where $\Delta\sigma$ is the difference between the cross sections of the two extreme isotopes and ΔN is the difference between the neutron numbers. These ratios for the Cr, Fe, Ni, and Zn isotopes are respectively 13.5 (13.5), 12.5 (13.0), 11.8 (12.3), 11.2 (11.7) (the values of the ratio $\Delta\sigma/\Delta N$ at deuteron energy 22.4 MeV are given in parentheses). The value of $\Delta\sigma/\Delta N$ calculated from the experimental reaction cross sections on Ni isotopes for 13.5-MeV deuterons is 34.7 ± 15.5, i.e., more than twice the theoretical values.

The theoretical cross sections for reactions on isotones with $N=26$, 28, 30, and 36 for 13.6-MeV and 22.4-MeV deuterons were calculated in Ref. 56 by Dubar' *et al.* by the optical model. The reaction cross sections on the isotones decrease with increasing Z at 13.6 MeV and remain practically constant at 22.4 MeV. Figure 15b shows the variation of the parameter r_0 calculated in accordance with Eq. (19) from the theoretical

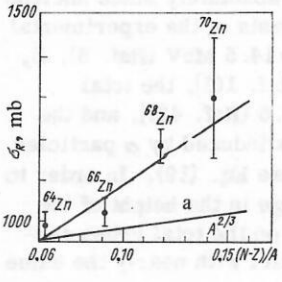

FIG. 14. Total cross sections of reactions on Zn isotopes as functions of the relative neutron excess in the nucleus (Ref. 63). The straight line is drawn through the experimental points; a) is the variation of the total reaction cross sections with the atomic weight of the target nuclei in a wide range of A.

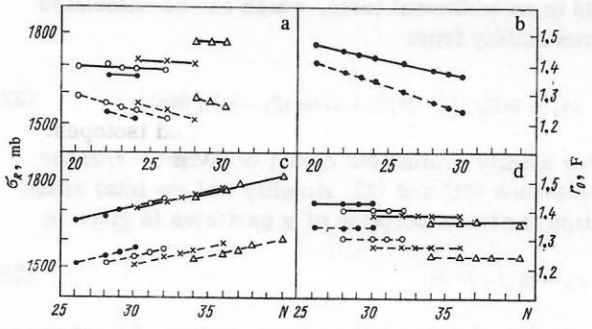

FIG. 15. Behavior of deuteron total reaction cross sections on isotopes and isotones calculated in the optical model (Ref. 56). a) Total reaction cross sections on isotones with $N=26$, 28, 30, 36 as functions of the number of protons Z in the nucleus; the black circles are isotones with $N=26$; the open circles, with $N=28$; the crosses, with $N=30$; the open triangles, with $N=36$. b) Dependence of the parameter r_0 obtained in accordance with Eq. (19) from analysis of the theoretical reaction cross sections. c) Total reaction cross sections on isotopes as functions of the number of neutrons N in the nucleus; the black circles are for Cr isotopes; the open circles for Fe isotopes; the crosses for Ni isotopes; and the open triangles for Zn isotopes. d) Parameter r_0 calculated by Eq. (19) on the basis of the theoretical reaction cross sections, as a function of N; the notation is the same as in Fig. 15c. In all cases the continuous lines are drawn through points corresponding to 22.4-MeV deuterons; the dashed lines, through points corresponding to 13.6 MeV.

reaction cross sections for these groups of isotones for 13.6-MeV and 22.4-MeV deuterons. As one would expect, at these two deuteron energies the Coulomb field of the nucleus has a strong influence on the parameter r_0. In the same way as we did in the investigation of isotopes, we introduce for the isotone straight lines the slope parameter $\Delta\sigma/\Delta Z$, where $\Delta\sigma$ is the difference in the cross sections for the two extreme isotones and ΔZ is the difference between the proton numbers. The ratio $\Delta\sigma/\Delta Z$ for isotones with $N=26$, 28, 30, and 36 is respectively $-12.5\,(-1.0)$, $-12.8\,(-1.7)$, $-14.0\,(-2.26)$, $-16.0\,(-4.0)$ for the deuteron energies 13.6 and 22.4 MeV (in parentheses). The minus sign indicates a decrease of the cross sections with increasing Z. The value of $\Delta\sigma/\Delta Z$ obtained on the basis of the experimen-

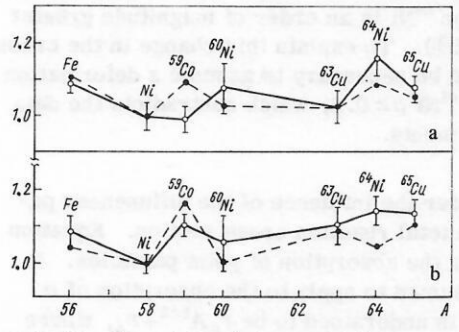

FIG. 16. Correlation between total cross sections of reactions induced by α particles (a) and deuterons (b) and excitation energy of the compound nucleus. The continuous lines join the experimental reaction cross sections; the dashed lines show the excitation energy.

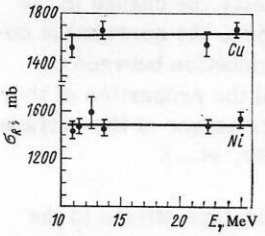

FIG. 17. Energy dependence of the deuteron total reaction cross sections on Ni and Cu nuclei.

tal data for 13.6-MeV deuterons is 60 ± 50 ($N=30$) and 47 ± 63 ($N=36$). Unfortunately, the errors in the determination of the reaction cross sections are still too large, so that quantitative estimates are hard to make.

Thus, although allowance for the influence of the Coulomb field of the nucleus on the nature of the variation of the total reaction cross sections in isotopes and isotones qualitatively reproduces the observed isotope–isotone effect, it does not explain the more rapid increase of the cross sections on isotopes compared with the general variation of cross sections as functions of A (see Fig. 8). To draw further conclusions, it will be necessary to consider in detail the connection between the total cross sections and the structure of specific nuclei. One could attempt to attribute the observed effect to the properties of the compound nucleus; these must be taken into account since the main contribution to the total reaction cross section at medium particle energies comes from inelastic processes accompanied by the formation of a compound nucleus.

In Fig. 16, we compare the variation of the total cross sections of reactions induced by deuterons and α particles with the excitation energy of the compound nucleus (the values are normalized to unity for the ^{58}Ni isotope). In some cases there is a clear correlation between the variations of the total cross sections and the excitation energy. The effect is to some extent related to the density of levels of the compound nucleus; this has the strongest dependence on the excitation energy. Since the total reaction cross sections are usually measured on fairly thick targets, there is an automatic averaging over an energy range of the order 0.5–1.0 MeV, i.e., over a very large number of levels of the compound nucleus. Because of the appreciable overlapping of these levels, there is no direct connection between the total cross section and the density of levels of the compound nucleus. This conclusion follows from the dependence of the deuteron total cross sections on the energy for Ni and Cu nuclei (Fig. 17). With increasing kinetic energy of the incident particles, the total reaction cross sections change little, whereas the density of levels of the compound nucleus increases exponentially. Nevertheless, a detailed investigation of the total cross sections as functions of the energy has not yet been made, and one cannot entirely eliminate the possibility of a connection between σ_R and the properties of highly excited states of the compound nucleus and, in particular, fluctuations in the density of levels.

The variation of the excitation energy from nucleus to nucleus is a consequence of the change in the binding

energy, i.e., essentially it reflects the change in the structure of the nuclei. Therefore, the correlation observed in Fig. 16 indicates a connection between the total reaction cross sections and the properties of the target nucleus in the ground state (shape of the surface, distribution of the nuclear density, etc.).

A possible explanation of the isotope effects in the total cross sections of reactions induced by deuterons and α particles was proposed in Ref. 64 by Dubar' *et al.* They consider the connection between the total cross sections of reactions induced by charged particles and the density distribution of the nuclear matter. To obtain information of this kind, they used the diffraction theory to analyze the cross sections of reactions on the isotopes ^{58,60,64}Ni with 27.2-MeV α particles, and the optical model of the nucleus to analyze the cross sections of reactions on the isotopes ^{58,60,64}Ni with 13.6-MeV deuterons.

Let us first consider the approximations on which equation (19) is based. First, it does not take into account the dependence on the Coulomb field of the nucleus. When it is used to analyze the variation of the total cross sections on isotopes of one element, this is not important, since correct allowance for the Coulomb interaction (for example, in the framework of the optical model) leads only to a renormalization of the constant r_0 without violating the relation (19). The constancy of r_0 for different isotopes and the renormalization effect when the energy of Z is changed is clearly illustrated by Fig. 15d. Second, Eq. (19) is valid for an absolutely black nucleus with a sharp boundary. In reality, the transparency of the nucleus is nonzero and there is a region near the surface in which it varies smoothly from a small value ε inside the nucleus to unity outside it. The theoretical absorption cross section obtained in the quasiclassical approximation is given by[65]

$$\sigma_R \approx \pi(1-\varepsilon^2)(R_0^2+\pi^2a^2/3)+2\pi(1-\varepsilon)^2 R_0 a, \tag{20}$$

where a is the diffuseness of the boundary of the nucleus. For an absolutely black nucleus ($\varepsilon = 0$) with sharp boundary ($a = 0$) the expression (20) is equal to the geometrical absorption cross section πR_0^2. The parameter R_0 in (20) corresponds to the distance from the center of the nucleus at which the transparency coefficient is 0.5.

Third, the expression (19) is valid for spherically symmetric nuclei. If the target nucleus is not spherical, its geometrical cross section will be greater than that of a spherical nucleus of equally large volume. If the nucleus has an ellipsoidal shape with small quadrupole deformation parameter β and nonsphericity γ, the absorption cross section for a point incident particle is given by[66]

$$\sigma_R = \pi R_0^2\{1+\beta^2[3+2\cos(2\gamma-\pi/3)]/8\pi\}. \tag{21}$$

Allowance for the finite size of the incident particle leads to an additional term, which can be calculated approximately from

$$\Delta\sigma_R \approx 2\pi R_0 r_\alpha\{1+\beta^2[25+14\cos(2\gamma-\pi/3)]/64\pi\}. \tag{22}$$

For axially symmetric nuclei ($\gamma = 0$ or $\gamma = \pi/3$) the expressions (21) and (22) simplify and the total cross section for the absorption of α particles is given by

$$\sigma_R = \sigma_R^0(1+\beta^2/2\pi), \tag{23}$$

where σ_R^0 is the absorption cross section of a spherical nucleus given by (19). As follows from (20) and (23), the diffuseness of the boundary of the nucleus and the nonsphericity of the nuclear shape increase the absorption cross section compared with values calculated from (19) for an absolutely black spherical nucleus with a sharp boundary. Analysis of data on the elastic scattering of electrons on separated isotopes of Ca (Ref. 67), Ni (Ref. 68), and Sn (Ref. 69) shows that the rms radius of the charge distribution does not increase faster when neutrons are added than follows from the $A^{1/3}$ proportionality law.

Since the radius of the neutron distribution is equal to the charge radius for light and medium nuclei,[69] it is reasonable in the framework of the model considered here to assume that the parameter r_0 is the same for the different isotopes. We define the ratio

$$\delta\sigma/\sigma \equiv (\sigma_R^e-\sigma_R^t)/\sigma_R^t, \tag{24}$$

which characterizes the deviation of the absorption cross section for a given isotope from the value σ_R^t calculated in accordance with Eq. (19) or (20) under the condition that none of the geometric parameters change for the various isotopes. One can then attempt to explain theoretically the value of $\delta\sigma/\sigma$ obtained experimentally: by an increase in the deformation parameter with increasing neutron number, by an increase in the diffuseness parameter, or by a joint influence of both factors.

It can be seen from (23) that for typical variations of the parameter β ($\beta = 0.1-0.2$) the expected increase in the absorption cross section does not exceed 0.8%, whereas the experimentally observed increment of the cross section on ^{64}Ni is an order of magnitude greater ($\delta\sigma/\sigma = 9.4\pm3.8\%$). To explain this change in the cross section it would be necessary to assume a deformation parameter for ^{64}Ni $\beta \geq 0.6$, which contradicts the data of other experiments.

Let us consider the influence of the diffuseness parameter on the total reaction cross section. Equation (20) is valid for the absorption of point particles. It can also be assumed to apply to the absorption of α particles if R_0 is understood to be $r_0A^{1/3}+r_\alpha$, where $r_\alpha = 1.1$ F is the half-density radius of the α particle. The variation of the absorption cross section on the transition from a nucleus with A nucleons to one with $A+n$ nucleons under the assumption that r_0 is constant

is given by

$$\Delta\sigma_R \equiv \sigma_R^{A+n} - \sigma_R^A \approx \frac{2}{3}\frac{n}{A}\pi R_0 (R_0 + a) + \left[\frac{2}{3}\pi^2 a + R_0\left(2 - 4\varepsilon + \frac{2}{3}\frac{n}{A}\right)\right]\pi\Delta a - 4\pi R_0 a \Delta\varepsilon, \quad (25)$$

where Δa and $\Delta\varepsilon$ are the changes in the diffuseness and the transparency of the nucleus when n nucleons are added, respectively; $R_0 = r_0 A^{1/3} + r_\alpha$.

It is known from the analysis of elastic scattering of α particles in accordance with the optical model that the parameter ε is of order 0.05. Assuming that it is constant for all the Ni isotopes, we can find Δa. The experimentally observed increase in the cross section of absorption on ^{64}Ni ($\delta\sigma/\sigma = 10.1 \pm 3.8\%$) can be explained by assuming that the diffuseness of the isotope ^{64}Ni is approximately 0.2 F greater than that of ^{58}Ni [$a = 0.57$ F for ^{58}Ni (Ref. 70) and $r_0 = 1.30$ F according to Eq. (19)].

The theoretical total reaction cross sections calculated in accordance with Eq. (20) as functions of the parameter a for the isotopes ^{58,60,64}Ni under the assumption that r_0 is constant ($r_0 = 1.30$ F) are shown in Fig. 18. The figure shows that agreement with experiment (the hatched strips) is achieved for the following values of the parameter a: 0.57 ± 0.10 F (^{58}Ni); 0.75 ± 0.20 F (^{60}Ni); 0.85 ± 0.10 F (^{64}Ni). The difference between the diffusenesses for ^{58}Ni and ^{64}Ni exceeds the experimental errors and is 0.28 ± 0.20 F. In reality, the change in the diffuseness may be somewhat less if the ^{64}Ni nucleus is less spherical than the ^{58}Ni nucleus. Thus, the increase in the experimental absorption cross section on isotopes, which exceeds what one expects from the increase in the radius of the nucleus when nucleons are added, can be explained by the greater diffuseness of the nuclear boundary. A qualitatively similar result is also obtained from analysis of the total deuteron cross sections of reactions on Ni isotopes in the framework of the optical model.

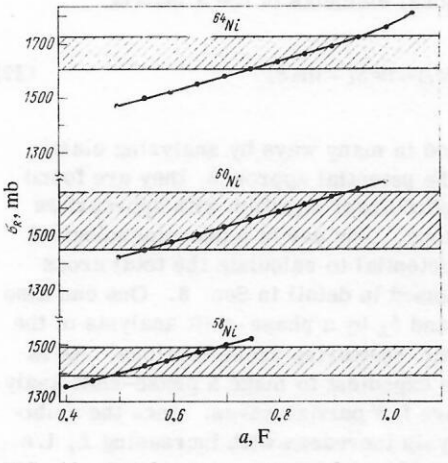

FIG. 18. Total cross sections of reactions induced by α particles on Ni isotopes as functions of the diffuseness parameter of the nuclear boundary. The hatched regions are the experimental values of σ_R (with allowance for experimental errors); the points are the result of calculation in the quasiclassical approximation.

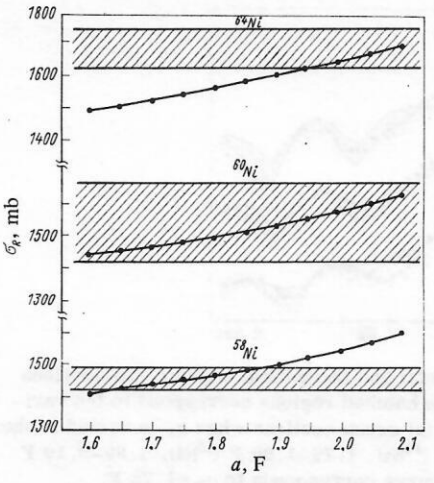

FIG. 19. Total reaction cross sections on Ni isotopes as functions of the diffuseness of the imaginary part of the optical potential. The hatched regions are the experimental values of σ_R (with allowance for the experimental errors); the points are the result of calculation by the optical model.

The calculations used the optical-potential parameters found earlier in Ref. 71 from an analysis of the elastic scattering of 13.6-MeV deuterons on Ni isotopes ($V = 72$ MeV, $W = 17$ MeV, $r_V = 1.35$ F, $r_W = 1.27$ F, $a_V = 0.73$ F, $a_W = 1.75$ F).

For the calculation of σ_R all the parameters of the potential were taken to be the same for all the investigated Ni isotopes except for the parameter a_W, which was varied in the range 1.6–2.1 F. Figure 19 shows σ_R as a function of a_W. The total reaction cross sections on the Ni isotopes can be described with the following values of the parameter a_W: 1.65–1.85 F (^{58}Ni); 1.6–2.1 F (^{60}Ni); 1.95–2.10 F (^{64}Ni). As can be seen from Fig. 19, it is impossible to reconcile the experimental and theoretical cross sections of reactions on the Ni isotopes if the parameter a_W has the same values. Agreement with experiment can be achieved by assuming that the isotope ^{64}Ni has a greater diffuseness than ^{58}Ni. Let us consider briefly the quality of the description of the differential cross sections of deuteron elastic scattering on Ni isotopes with the sets of potential parameters which have been found. The experimental and theoretical angular distributions of deuteron elastic scattering on the Ni isotopes are shown in Fig. 20. The hatched regions correspond to the variation of the differential cross sections when the parameter a_W is varied in the range 1.65–1.75 F (^{58}Ni), 1.75–1.90 F (^{60}Ni), 1.90–2.10 F (^{64}Ni). The remaining parameters have fixed values for all the Ni isotopes. The sets of optical-potential parameters found can be regarded as suitable for simultaneous description of elastic scattering and the total reaction cross sections on Ni isotopes.

The value of the ratio $\delta a = a(^{64}\text{Ni})/a(^{58}\text{Ni})$ obtained by

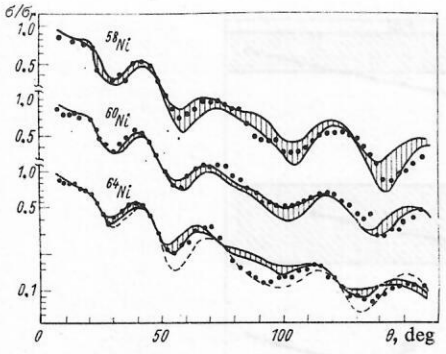

FIG. 20. Experimental and theoretical angular distributions for Ni isotopes. The hatched regions correspond to the variation of the differential cross sections when a_W is varied in the ranges 1.65–1.75 F (^{58}Ni), 1.75–1.90 F (^{60}Ni), 1.90–2.10 F (^{64}Ni). The dashed curve corresponds to $a_W = 1.75$ F.

analyzing the experimental deuteron reaction cross sections by the optical model ($\delta a = 1.23 \pm 0.14$) agrees well with the ratio obtained by analyzing the absorption cross sections of α particles by the diffraction model ($\delta a = 1.49 \pm 0.35$). Let us compare the ratios of the diffuseness for the Ni isotopes that we have found with those obtained by analyzing the elastic scattering of electrons on the same isotopes.[72] The diffuseness of ^{64}Ni is approximately 2% greater than that of ^{58}Ni, which is appreciably smaller than the ratio we obtained. The radii of the nuclei found from electron scattering on Ni isotopes[72] are described by the relation $R = r_0 A^{1/3}$ to within 1%. The diffuseness obtained from the analysis of electron elastic scattering characterizes the decrease of the proton density at the nuclear boundary. Therefore, the difference between the diffusenesses observed for the Ni isotopes on the basis of electron elastic scattering and the total reaction cross sections can be attributed to the existence of a more spread out distribution of the neutron density in the surface layer of the nucleus. Many other experimental facts confirm this conclusion. The experimental data on deuteron breakup as a result of collision with Ni isotopes[73] also indicate that the ^{64}Ni isotope is more diffuse than ^{58}Ni. An earlier analysis of the differential cross sections for elastic scattering of 13.6-MeV deuterons on even Ni isotopes[61] had shown that to explain the absolute magnitude of the elastic scattering on ^{58}Ni it is necessary to reduce the parameter a compared with its value for the other isotopes. Similar isotope effects are revealed by the analysis of scattering of 6.5-MeV deuterons on Ni and Zn isotopes.[62]

The conclusion that the nuclear surface may become more diffuse when neutrons are added can also be drawn from an analysis of the averaged parameters of the optical potential as a function of the neutron excess $(N - Z)/A$. This question is discussed in detail in Sec. 8. Here we merely mention the work of Kashuba and Kozin,[74] who analyzed the differential cross sections of elastic scattering, the total interaction cross sections, and the polarization for neutrons with energy of about 4 MeV on 20 elements from Al to U. They obtained the following expression for the diffuseness of the real part of the optical potential:

$$a = [0.568 + 0.813\,(N - Z)/A]\ \text{F}. \tag{26}$$

This dependence characterizes the variation of a not only on the transition from element to element but also when the number of neutrons in the isotope changes. In this case, because Z is constant but N and A change, the dependence is more clearly expressed. Relations analogous to (26) but for the diffuseness of the imaginary part of the potential were obtained later by analyzing neutron and proton data over a wide energy range[51,53,54] (see Sec. 8).

It is interesting to note that representation of the total reaction cross sections as functions of $(N - Z)/A$ and not as functions of A (or $A^{2/3}$) "regularizes" to a considerable extent the law of variation of σ_R on the transition from nucleus to nucleus. To see this, it is sufficient to compare the data shown in Figs. 11 and 16. This can serve as an additional indication that there is a direct connection between the total cross section and the diffuseness of the nuclear surface.

Thus, the collection of experimental data for Ni isotopes can be successfully interpreted by assuming that the radii of the isotopes satisfy the usual law $R = r_0 A^{1/3}$, whereas the diffuseness increases on the transition from a light to a heavier isotope, this being due to the change in the neutron density in the boundary layer of the nucleus. In all probability, a similar situation obtains for other isotopes.

7. USE OF PHASE SHIFTS TO CALCULATE THE TOTAL REACTION CROSS SECTIONS

When the method of partial waves is used, the main formula for calculating the total reaction cross sections is (4). The diagonal elements of the S matrix

$$S_L = |S_L| \exp(i2\delta_L) = \text{Re}\, S_L + i\,\text{Im}\, S_L \tag{27}$$

can be determined in many ways by analyzing elastic scattering. In the potential approach, they are found by solving the Schrödinger equation with appropriate boundary conditions. The use of a phenomenological complex pseudopotential to calculate the total cross sections is discussed in detail in Sec. 8. One can also determine $|S_L|$ and δ_L by a phase-shift analysis of the differential elastic-scattering cross sections. As is well known, it is expedient to make a phase-shift analysis when there are few partial waves, since the ambiguity of the analysis increases with increasing L, i.e., with increasing energy E of the particles. The point is that at low energies one can fairly often take into account only the real phase shifts δ_L, assuming $|S_L| = 1$. This halves the number of phase shifts. It is a consequence of this approximation that the theoretical total

reaction cross section is zero, which contradicts experiments. If one goes over to complex phase shifts (see, for example, Refs. 90–92), the phase shifts are not determined uniquely and, as a consequence, there is an uncertainty in the value of the theoretical total reaction cross section. It is therefore not surprising that phase shifts which parametrize differential cross sections splendidly can predict total reaction cross sections very different from those measured experimentally (see the dashed curve in Fig. 21). Thus, the experimental total reaction cross sections are more often used to reduce the ambiguity of phase-shift analysis than phase-shift analysis of elastic scattering is used to calculate total cross sections.

To reduce the ambiguity of phase-shift analysis, one can postulate a functional dependence of $|S_L| \equiv \eta_L$ and σ_L on L of the type

$$\eta_L = \eta(L, p_i), \tag{28}$$

$$\delta_L = \delta(L, p_i), \tag{29}$$

or equivalently,

$$\mathrm{Re}\, S_L = \varphi(L, p_i); \tag{30}$$

$$\mathrm{Im}\, S_L = \psi(L, p_i), \tag{31}$$

and regard L as a continuous argument in the range $[0, \infty]$. The constants p_i in (28)–(31) are free parameters that ensure the best approximation of η_L and δ_L (or $\mathrm{Re}S_L$ and $\mathrm{Im}S_L$) at the points $L = 0, 1, 2, \ldots$. The procedure for finding the functional dependences (28)–(31) and the values of the constants p_i by analyzing the experimental reaction cross sections is known as parametrized phase-shift analysis (PPA). This method has been widely used to analyze differential cross sections of elastic scattering for various types of particles.

After the classical investigation of Akhiezer and

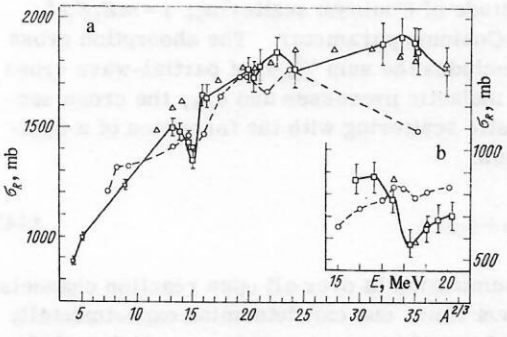

FIG. 21. Comparison of experimental total cross sections of reactions induced by α particles with theoretical values calculated by the optical model and PPA. The open squares are the experiment, the open circles the PPA calculation, the open triangles the optical-model calculation. a) Values of σ_R taken from Ref. 44 for 40-MeV α particles; σ_R^T data taken from Refs. 56 and 83. b) Energy dependence of the total cross sections of reactions induced by α particles on the ^{12}C nucleus.[46]

Pomeranchuk,[75] who used a one-parameter representation of the S matrix in the form

$$S_L = \begin{cases} 0 & L < L_0; \\ \exp(2i\sigma_L) & L > L_0, \end{cases} \tag{32}$$

a large number of different types of functional dependences (28)–(31) were proposed. Many of them are considered in the reviews Refs. 76 and 77, and also in the papers of Inopin *et al.*[78–81]

If there are only a few free parameters (up to five), one can explain perfectly satisfactorily the angular distributions in the range of angles $\theta \leq 60°$ using comparatively simple analytic expressions for calculation of the cross sections. The possibilities of using PPA to calculate the total reaction cross sections have not yet been sufficiently investigated. We shall distinguish two cases: 1) the analytic, when a simplified choice of the parametrization (28)–(31) enables one to calculate the series (4) analytically, and 2) the numerical. In Ref. 77 with a three-parameter representation of the S matrix:

$$\mathrm{Re}\, S_L = \varphi(L, L_0, \Delta); \tag{33}$$

$$\mathrm{Im}\, S_L = b\, \partial\varphi/\partial L, \tag{34}$$

where

$$\varphi(L, L_0, \Delta) = \{1 + \exp[(L - L_0)/\Delta]\}^{-1}, \tag{35}$$

the following simple expression is obtained for the absorption cross section:

$$\sigma_R = \pi \left(\frac{L_0}{k}\right)^2 \left[1 + \frac{\pi}{3}\left(\frac{\Delta}{L_0}\right)^2\right] - \frac{\pi}{3k^2}\frac{L_0}{\Delta} b^2, \tag{36}$$

where L_0, Δ, and b are parameters found by analyzing the differential cross sections of elastic scattering.

To calculate the total cross sections of reactions on ^{27}Al induced by 27.2-MeV α particles Eq. (36) was used. From an analysis of the differential elastic-scattering cross sections the following parameters were obtained: $L_0 = 11.5$, $\Delta = 0.62$, and $b = 1.08$, which correspond to $\sigma_R = 1000$ mb, about 13% smaller than the experimental value. Bearing in mind the simple form of Eq. (36) and the absence of free parameters, this result can be regarded as entirely satisfactory. If we use the exact Eq. (4) and five-parameter representations of the S matrix in the form

$$\mathrm{Re}\, S_L = \varphi(L, L_{01}, \Delta_1); \tag{37}$$

$$\mathrm{Im}\, S_L = b\, \frac{\partial\varphi(L, L_{02}, \Delta_2)}{\partial L_{02}}, \tag{38}$$

then in the same case we obtain $\sigma_R = 1211$ mb, i.e., about 7% more than the experimental value. The parameters $L_{01} = 11.31$, $L_{02} = 11.75$, $\Delta_1 = 0.74$, $\Delta_2 = 0.70$, and $b = 1.08$ are determined from an analysis of elastic scattering.[82]

The parametrizations (37) and (38) were used to calculate the total cross sections of reactions induced by α particles with energy 39–44 MeV in Ref. 83 by Gonchar and Zheltonog, who used the PPA to analyze elastic scattering of α particles on a large number of nuclei. The results of the calculations are compared with the Igo and Wilkins experimental cross sections[44] at $E_\alpha = 40$ MeV in Fig. 21. It can be seen that in many cases the discrepancy between the PPA calculations and experiment appreciably exceeds the experimental errors.

When a sufficiently large number of free parameters are used in PPA one can achieve a detailed description of the experimental data for elastic scattering and the total cross sections. These parameters must be found by minimizing a functional of the type

$$\chi^2 = \frac{1}{N}\sum_{i=1}^{N} \omega_i [\sigma^t(\theta_i) - \sigma^e(\theta_i)]^2 + \omega_R [\sigma_R^t - \sigma_R^e], \quad (39)$$

where N is the number of experimental points in the angular distribution, $\sigma(\theta)$ are the differential cross sections of elastic scattering, and ω_i are certain weight factors. The purely computational problems in this case are about as great as those involved in the numerical integration of the Schrödinger equation with an optical interaction potential. At the same time, for the same number of free parameters, the optical model describes the differential cross sections of elastic scattering in a wider range of angles than the PPA; therefore, for numerical methods it is better to use the optical model for simultaneous analysis of the differential and the total cross sections.

8. THE OPTICAL MODEL AND TOTAL REACTION CROSS SECTIONS

The many-parameter potential of the optical model currently used to describe scattering and nuclear reactions explains a large number of experimental facts. However, any physical experiment determines only a certain region in the parameter space, and the boundary of this region is diffuse because of the errors of the experimental data. Therefore, several experiments must be carried out if unique results are to be obtained. Such experiments include ones to determine the differential and total reaction cross sections and polarization. The parameter regions determined by means of each of these experiments may overlap partly, enabling one to obtain unambiguous information about the parameters and the form of the potential. On the other hand, it is very helpful to have sets of parameters that enable one to find, and possibly predict, observable experimental values with a fairly high accuracy.

The optical potential currently used has the form

$$U(r) = V_c(r) - V f_s(x) - i[W_s f(x) + W_{D(G)} f_{D(G)}(x)] + V_{s0}(r)\,\mathbf{LS}, \quad (40)$$

where

$$f_s(x) = (1+\exp x)^{-1};$$

$$f_D(x) = -4a\frac{d}{dr} f_s(x);$$

$$f_G(x) = \exp(-x^2);$$

$$V_{s0}(r) = \left(\frac{\hbar^2}{m_\pi c}\right)^2 V_{s0}\frac{1}{r}\cdot\frac{d}{dr} f_s(x);$$

$$x = (r - r_0 A^{1/3})/a,$$

$V_c(r)$ is the Coulomb potential of the interaction between the incident particle and the nucleus; V and W are the depths of the real and the imaginary parts of the potential; $f_s(x)$ is the Woods–Saxon form factor; $f_{D(G)}(x)$ is the form factor of the imaginary part in the form of the derivative of the Woods–Saxon form factor (or in the form of a Gaussian function); r and a are the radius and diffuseness parameters, respectively [in the general case, they are different for different components of the potential (40)]. The last term in (40) determines the spin–orbit interaction of the incident particle with the nucleus (S-spin operator; L is the orbital angular momentum of the incident particle). In what follows, to shorten the expression of the potential (40), we shall specify only the subscripts of the function $f(x)$ in (40) and the number of free parameters of the central nuclear potential. For example, the optical potential with surface absorption in the form (40) and with different geometrical parameters for the real and the imaginary parts will be denoted by $SD6$, etc.

The differential cross sections and the absorption cross sections can be calculated by means of the relations

$$\frac{d\sigma}{d\Omega} = |A(\theta)|^2; \quad (41)$$

$$\sigma_a = \frac{\pi}{k^2}\sum_{L=0}^{\infty}(2L+1)(1-|S_L|^2); \quad (42)$$

$$A(\theta) = A_c(\theta) + \frac{1}{2ik}\sum_{L=0}^{\infty}(2L+1)(S_L - 1)\exp(2i\sigma_l)\,P_L(\cos\theta), \quad (43)$$

where $A_c(\theta) = (-\gamma/2k)\,\mathrm{cosec}^2(\theta/2)\exp(2i\sigma_0 - 2i\gamma\ln\sin\theta/2)$ is the amplitude of Coulomb scattering; $\gamma = mZ_1Z_2e^2/(k\hbar)^2$ is the Coulomb parameter. The absorption cross section σ_a includes the sum $\sum_{i=1}^{N}\sigma_i$ of partial-wave cross sections of inelastic processes and σ_{CE}, the cross section for elastic scattering with the formation of a compound nucleus:

$$\sigma_a = \sum_{i=1}^{N}\sigma_i + \sigma_{CE}, \quad (44)$$

where the summation is over all open reaction channels. At the present time, one can determine experimentally only the total reaction cross section σ_R, which includes the sum $\sigma_R = \sum_{i=1}^{N}\sigma_i$ of the cross sections of the inelastic processes. At the same time, the absorption cross section σ_a can be calculated theoretically. This situation makes it difficult to compare the experimental data with calculations by the optical model at low energies, for which the cross section of elastic scattering through a compound nucleus, σ_{CE}, is large.

The optical model is successfully used to describe elastic scattering and polarization of protons and the elastic scattering of deuterons and α particles. Unfortunately, the sets of optical-parameter potentials obtained are not unique. There are two types of ambiguity in the real part of the optical potential: a) a continuous ambiguity for which a small change of one parameter can be compensated by a change of the others; b) a discrete ambiguity for which at a given radius of the real part of the potential good agreement is observed with a family of potential depths. There is also an ambiguity in the choice of the imaginary part of the optical potential, this being inherent for all types of particles.

When the first experimental determinations of total reaction cross sections were published, analysis by the optical model in the energy range 10–100 MeV was basically restricted to elastic scattering of protons and the neutron total cross sections. However, the analysis of Saxon and Glassgold[14,15] already indicated that it was necessary to include in the optical-model analysis of the proton total cross sections an additional experiment capable of reducing the ambiguity in the optical-potential parameters and choosing the form factor of the imaginary part of the potential.

As follows from (5), the total reaction cross section determines the imaginary part of the potential. However, this does not mean that the parameters of the real part of the potential are unimportant for analysis of the experimental data on total reaction cross sections: In the framework of the optical model, elastic scattering and absorption are inseparably linked and must be described by one and the same potential. Thus, σ_R must be calculated at the same time as $d\sigma/d\Omega$ and, comparing both values with experiment, one must find the optimal optical-potential parameters by successive approximations.

Proton total reaction cross sections. During the last few years, a systematic study has been made of the elastic scattering and polarization of protons in the energy range 9–60 MeV (Refs. 51, 53, and 54). Unique optical-potential parameter sets have been found capable of describing the experimental data on elastic scattering and polarization in a wide range of energies and atomic weights. However, in the majority of cases the information obtained is on the real part of the optical potential and the spin–orbit potential.

On the other hand, Perey's detailed analysis[30] of elastic scattering of protons with energy 9–22 MeV shows that allowance for the dependence on $(N-Z)/A$ in the real part of the optical potential enables one to explain elastic scattering and polarization well but not the experimentally observed reaction cross sections.

From an analysis of the differential cross sections of elastic scattering and polarization in the proton energy range 30–61.4 MeV (Refs. 53 and 54) the following expression is found for the real part of the optical potential:

$$V = 49.9 - 0.22E_p + 0.4Z/A^{1/3} + 26.0\,(N-Z)/A.$$

Let us turn to an analysis of the information obtained on the basis of the optical model with inclusion of experimental data on the total reaction cross sections.

Becchetti and Greenlees[51] made a global search for optical-potential parameters in the proton energy range 10–40 MeV on the basis of experimental data on elastic scattering [40 values of $\sigma(\theta)$], polarization [28 values of $P(\theta)$], and total reaction cross sections (eight values of σ_R). The inclusion of the experimental total reaction cross sections in the analysis was helpful from the point of view of making more precise the parameters W_S, r_W, and a_W as functions of A and E. To describe the reaction cross sections, it was found to be best to introduce a term proportional to $(N-Z)/A$ in the diffuseness of the imaginary part of the optical potential. The search yielded the following expressions for the parametrization of V, W_S, W_D, and a_W:

$$\left.\begin{aligned} V &= 54.0 - 0.32E_p + 0.4Z/A^{1/3} + 24.0\,(N-Z)/A;\\ W_S &= 0.22E_p - 2.7;\\ W_D &= 11.8 - 0.25E_p + 12.0\,(N-Z)/A;\\ a_W &= 0.51 + 0.7\,(N-Z)/A. \end{aligned}\right\} \qquad (45)$$

Becchetti and Greenlees[51] also analyzed the experimental data on the elastic scattering of neutrons [30 values of $\sigma(\theta)$], the polarization [four values of $P(\theta)$], and total cross sections (28 values of σ_T) in the neutron energy range up to 24 MeV. The parametrizations of W_S and W_D obtained from the best agreement with the neutron data have the form

$$\left.\begin{aligned} W_S &= 0.22E_n - 1.56;\\ W_D &= 13.0 - 0.25E_n - 12.0\,(N-Z)/A. \end{aligned}\right\} \qquad (46)$$

In Ref. 51, Becchetti and Greenlees obtained an expression for the real part of the optical potential giving a good description of the neutron and proton data:

$$\left.\begin{aligned} V_n &= 55.2 - 0.32E_n - 24.0\,(N-Z)/A;\\ V_p &= 55.2 - 0.32E_p - 24.0\,(N-Z)/A + 0.27Z/A^{1/3}. \end{aligned}\right\} \qquad (47)$$

The influence of the total reaction cross sections on the choice of the depth of the imaginary part of the optical potential as a function of the energy and the nuclear symmetry term in the proton energy range 30–61.4 MeV was investigated in Ref. 33. Figure 22 shows the dependence of $W_D a_W$ on the $(N-Z)/A$ term found from analysis of elastic scattering, polarization, and total reaction cross sections at the proton energies 30, 40, and 61.4 MeV. There is a clear tendency for $W_D a_W$ to increase with $(N-Z)/A$. Since the absorption on the nuclear surface is proportional to $W_D a_W$, a dependence on $(N-Z)/A$ can be included either in W_D (Refs. 30

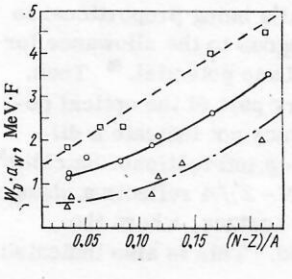

FIG. 22. Dependence of $W_D a_W$ on the $(N-Z)/A$ term for description of elastic scattering, polarization, and total reaction cross sections for protons of energy 30 MeV (open squares), 40 MeV (open circles), and 61.4 MeV (open triangles). Data taken from Ref. 33.

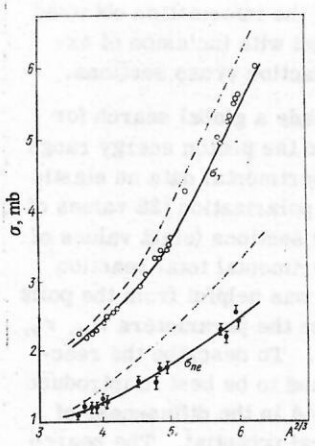

FIG. 23. Measured and predicted total cross sections and cross sections for inelastic scattering of 24-MeV neutrons. Data taken from Ref. 84. The continuous curve is calculated with $W_D^{(-)}$; the dashed curve, with $W_D^{(+)}$.

and 84) or in a_W (Ref. 51). The following parametrization of W_S, W_D, and a_W was obtained on the basis of the analysis:

$$\left.\begin{aligned} W_S &= 1.2 + 0.09E_p; \\ W_D &= 4.2 - 0.05E_p + 15.5\,(N-Z)/A; \\ a_W &= 0.74 - 0.08E_p + 1.0\,(N-Z)/A. \end{aligned}\right\} \qquad (48)$$

Comparison of (45) and (48) shows that the use of total reaction cross sections to parametrize the parameters of the imaginary part of the optical potential leads to a more accurate energy dependence of W_S and W_D: With increasing energy, the volume part of the potential increases while the surface part decreases. It also follows from the analysis that the diffuseness of the imaginary part depends on the energy: With increasing energy the diffuseness decreases.

Satchler,[84] who analyzed scattering of 24-MeV neutrons with an optical potential taken from analysis of the scattering of 30-MeV protons, showed that the total cross sections and the cross sections of inelastic processes have a greater influence on the choice of W_D as a function of $(N-Z)/A$ than the differential cross sections of elastic scattering.

It follows from a comparison of (45) and (46) for W_D values obtained, respectively, from analysis of the proton and neutron data that they are virtually the same except for the sign in front of the $(N-Z)/A$ term. The influence of the choice of the sign in front of the $(N-Z)/A$ term in $W_D^{(\pm)}$ on the description of the total cross sections and cross sections of inelastic processes for 24-MeV neutrons was investigated by Satchler.[84] The results are shown in Fig. 23, from which it can be seen that both processes can be described successfully only with $W_D^{(-)}$. A similar result was obtained by Menet *et al.*,[33] who used the parametrization (48) to describe the neutron data. This can be interpreted as a consequence of the complex potential's being proportional to the term $(\mathbf{t}\cdot\mathbf{T})$, which is analogous to the allowance for the isospin dependence in the Lane potential.[93] Thus, the dependence of the imaginary part of the optical potential on the $(N-Z)/A$ term does not indicate a difference between the n–p and p–p interactions. Satchler[85] notes that the dependence on $(N-Z)/A$ reflects a change in the geometry of the nuclear surface, where the greatest absorption is observed. This is also indicated by the results of Dubar' *et al.*,[64] who investigated isotope effects in the total cross sections of reactions induced by deuterons and α particles, and also by the dependence of σ_R on $(N-Z)/A$ discussed in Secs. 5 and 6.

A global investigation of the parameters of the imaginary part of the optical potential as functions of the energy and the nuclear symmetry term has not been made for other types of particle. A similar analysis based on experimental data for the total cross sections of reactions induced by deuterons and α particles is at present impossible because data in a wide range of energies and atomic weights are not available.

Deuteron total reaction cross sections. In Ref. 43, Dubar' *et al.* compared the experimental deuteron total cross sections with theoretical values obtained by analyzing differential cross sections of elastic scattering[71] on the basis of the unique[55] and optimal sets of optical potentials. Whereas the cross sections calculated with the former only qualitatively reproduce the behavior of the experimental cross sections, when optimal parameters are used it is possible to reconcile the experimental and theoretical cross sections for virtually all the analyzed nuclei.[41,43] Agreement with experiment is achieved basically by changing parameters in the optical potential such as W, r_W, and a_W. It is helpful to use the experimental deuteron total reaction cross sections to reduce the sets of optical-potential parameters. In particular, the experimentally obtained values of σ_R for Fe and ^{63}Cu nuclei can be explained by means of just one optical-potential set, whereas Vereshchagin *et al.*[71] gave 11 sets for Fe and three for ^{63}Cu. The value of σ_R on ^{64}Ni is described by eight sets of the 24 given. The region of continuous ambiguity for the Ni and Fe nuclei could be reduced by eliminating the potentials with $a_V \geqslant 0.74$ F. Further, none of the optical-potential sets given in Ref. 71 for ^{59}Co and ^{65}Cu (eight for ^{59}Co and three for ^{65}Cu) can explain the experimental value of σ_R. The analysis[43] of Dubar' *et al.* indicates, in particular, the need to obtain experimental data with a high accuracy. Thus, for the ^{60}Ni nucleus (error of determination about 8%) all the 18 sets given in Ref. 71 are equally suitable for explaining σ_R.

The sensitivity of the total reaction cross sections to the choice of the form factor for the imaginary part of the optical potential can be seen in the example of ^{64}Ni. In Ref. 71, there are optimal parameters of the type SS4 and SG6 for ^{64}Ni. The absorption cross sections with optimal parameters of the SS4 type are approximately 21% smaller than σ_R (error 4%). Optical potentials of the SG6 type describe the experimental value of the cross section satisfactorily.

It has also been found helpful to use the total reaction cross sections to investigate the discrete ambiguity. Thus, the so-called shallow optical potentials, for which $V \lesssim 30$ MeV, predict in all investigated cases (^{63,65}Cu, ^{59}Co, ^{64}Ni) theoretical cross sections smaller than the experimental by about 15% on the average (the error in the determination of the cross sections is 5, 4, 3, and 4%, respectively). Thus, it follows from Ref. 43 that to describe the total reaction cross sections for 13.6-MeV deuterons four-parameter optical potentials

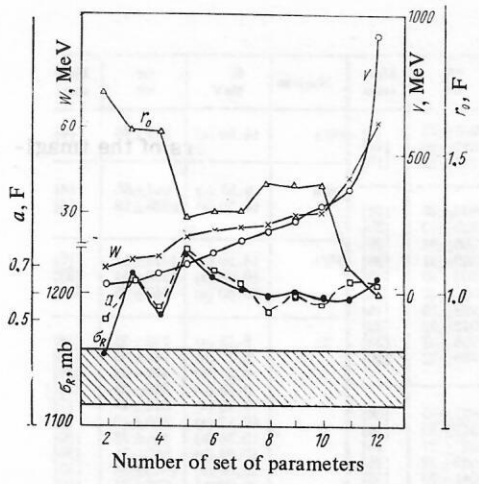

FIG. 24. Theoretical total cross sections of reactions on the Al nucleus as functions of the optical-potential parameters (volume absorption). The hatched region corresponds to the experimental value of σ_R (with allowance for experimental errors); the black circles show σ_R^T, the open squares a, the crosses W (left-hand scale), the open circles V, the open triangles r_0 (right-hand scale).

with volume absorption and shallow six-parameter potentials are unsuitable.

Total cross sections of reactions induced by α particles. When elastic scattering of α particles is analyzed by the optical model, one obtains a discrete ambiguity in the choice of the depth for the real part of the potential and a continuous ambiguity of the type $Vr_V^2 = \text{const}$. If the real and the imaginary potential have the same geometrical parameters, there is a preference for taking a potential with volume absorption, this leading in the calculation of $d\sigma/d\Omega$ to better agreement with experiment in the region of forward scattering angles. If the real and imaginary potentials have different geometrical parameters, the description of the angular distributions of elastic scattering is more or less equally good with volume or surface absorption.

We now consider the information obtained by comparing the experimental total reaction cross sections with the theoretical ones calculated by the optical model. The change of the theoretical reaction cross sections on ^{27}Al resulting from a change of the optical-potential parameters (a four-parameter potential was used) is shown in Fig. 24. A clear correlation is observed only between the total cross sections and the diffuseness parameter: σ_R increases with increasing diffuseness. However, as can be seen from Fig. 24, agreement with experiment is obtained with only one optical-potential set. Analysis of the total cross sections of reactions induced by 27.2-MeV α particles[43] showed that a potential allowing for volume and surface absorption is better suited to the description of reaction cross sections on the ^{27}Al nucleus. It follows from the analysis in Ref. 43 of the total reaction cross sections on nuclei of medium atomic weight with 27.2-MeV α particles that the use of four- and six-parameter potentials with volume absorption does not, in the majority of cases, lead to agreement with the experimental cross sections, although the differential cross sections of elastic scattering are described perfectly well by such potentials.

Simonov, Terenetskiĭ, and Tokarevskiĭ[86] compared in detail potentials of the type SS4 and SD4 corresponding to eight discrete regions of continuous ambiguity in the range of variation of V from 40 to 300 MeV for the description of the elastic scattering of 27.2-MeV α particles on ^{60}Ni. Comparison of the theoretical total cross sections which they calculated[86] with the experimental[43] measurement of σ_R shows that satisfactory agreement exists only for a potential of the type SD4. The theoretical cross sections calculated with the potential SS4 are smaller than the experimental values for all discrete sets. However, the angular dependence of the differential cross sections can be parametrized better by the potential SS4, and this emphasizes once more the need to analyze both experiments simultaneously in order to obtain realistic information about the optical potential.

CONCLUSIONS

The measurement of total reaction cross sections during the last 10–15 years has developed into a fruitful direction of nuclear physics, making it possible to obtain important information about the sizes of nuclei, the distribution in them of nuclear matter, the variations of these characteristics for isotopes and isotones, etc. Since these parameters reflect the detailed structure of nuclei, their measurement is very important for the further development of our ideas about nuclear structure.

It is very important to measure the total cross sections and select the most suitable parameters of the optical potential; this has independent value and is also important for the successful use of the distorted-wave method and the coupled-channel method. Thus, a further development of this direction will foster the development of the theory of the nucleus and the theory of nuclear reactions. If data on total reaction cross sections are to be used successfully for these purposes, it is important to reduce the error in the measurement of the total cross sections to 1% or less. One of the main experimental tasks here is the development of precise methods for determining the thicknesses of targets.

It is necessary to continue measurements of the total reaction cross sections on targets of separated isotopes and especially of the excitation functions, which enable one to obtain data about the density distribution in the surface layer of the nucleus. It is desirable to set up experiments on the same target nuclei with different types of particle and evaluate them simultaneously with a view to obtaining consistent results. It is of great interest to include the total reaction cross sections in the global search for unique parameters of the optical potential of composite particles. At the present time, there is an acute shortage of experimental data suitable for this purpose.

Among the unresolved problems, it is particularly important to eliminate the blanks in the investigation of the total reaction cross sections. Above all, it is necessary to develop methods for calculating total cross

sections with allowance for structure of the colliding nuclei. Such methods are needed to interpret the experiments already performed with deuterons and ^{4}He ions and they will be even more necessary when new experiments to measure total cross sections of reactions induced by heavy ions are undertaken. We also mention the absence of experimental data for the total cross sections of reactions induced by tritons.

APPENDICES

Proton total reaction cross sections

Nucleus	E, MeV	σ_R, mb	Literature
Be	9.93 (a)	633±14	[7]
	10.15 (a)	663±14	[7]
	16.20 (a)	571±18	[38]
	17.00 (a)	599±17	[38]
	18.50 (a)	555±15	[38]
	20.00 (a)	542±15	[38]
	21.90 (a)	530±16	[38]
	24.20 (a)	519±17	[38]
	26.60 (a)	484±17	[38]
	28.00 (a)	474±13	[38]
	99.30 (б)	231±7	[10]
C	9.88 (a)	195±47	[37]
	9.94 (a)	229±19	[7]
	10.16 (a)	332±19	[7]
	10.20 (a)	181±53	[37]
	10.40 (a)	434±58	[37]
	10.72 (a)	318±61	[37]
	13.51 (a)	207±39	[37]
	13.77 (a)	380±43	[37]
	14.54 (a)	324±42	[37]
	14.79 (a)	235±40	[37]
	16.20 (a)	430±16	[87]
	16.48 (a)	382±32	[31]
	17.30 (a)	431±17	[87]
	17.41 (a)	343±24	[37]
	18.60 (a)	417±17	[87]
	19.46 (a)	401±24	[37]
	19.90 (a)	438±17	[87]
	21.10 (a)	448±17	[87]
	21.80 (a)	441±21	[87]
	22.00 (d)	420±42	[88]
	23.80 (a)	435±18	[87]
	25.00 (d)	376±40	[4]
	25.30 (a)	416±19	[87]
	26.40 (a)	378±18	[87]
	28.00 (a)	396±13	[87]
	29.00 (a)	418±18	[25]
	30.00 (a)	447±20	[33]
	34.00 (a)	445±20	[3]
	40.00 (a)	371±11	[33]
	42.00 (d)	405±35	[88]
	49.50 (a)	345±13	[33]
	54.00 (d)	355±50	[4]
	60.80 (a)	310±13	[33]
	61.00 (a)	200±13	[16]
	99.30 (b)	245±7	[10]
	134.00 (a)	220±24	[89]
F	99.10 (b)	353±10	[10]
Mg	9.15 (a)	602±25	[29]
	16.47 (a)	712±56	[31]
	99.10 (b)	399±12	[10]
^{27}Al	8.80 (a)	674±45	[28]
	8.87 (b)	650±26	[36]
	9.37 (b)	650±26	[36]
	9.85 (c)	741^{60}_{30}	[18]
	9.88 (b)	594±26	[36]
	9.90 (a)	656±28	[7]
	10.12 (a)	704±28	[7]
	10.39 (b)	610±26	[36]
	16.29 (a)	701±34	[31]
	29.00 (a)	775±37	[25]
	34.00 (a)	600±42	[3]
	40.00 (a)	645±35	[33]
	60.80 (a)	499±27	[33]
	61.00 (a)	392±25	[16]
	99.40 (b)	430±12	[10]
	134.00 (a)	373±37	[89]
Ca	10.34 (a)	505±59	[37]
	11.38 (a)	736±54	[37]
	12.42 (a)	717±63	[37]
	12.42 (a)	742±67	[37]
Ca	13.45 (a)	931±46	[37]
	13.46 (a)	953±50	[37]
	13.97 (a)	883±44	[37]
	14.48 (a)	920±47	[37]
	14.97 (a)	822±35	[37]
	15.51 (a)	766±39	[37]
	16.49 (a)	765±35	[37]
	17.51 (a)	850±34	[37]
	18.54 (a)	821±35	[37]
	19.55 (a)	806±33	[37]
	20.57 (a)	861±34	[37]
	21.59 (a)	871±32	[37]
	28.50 (a)	913±38	[26]
	99.70 (b)	580±17	[10]
Sc	6.75 (c)	433±57	[27]
	99.30 (b)	634±18	[10]
Ti	9.15 (a)	750±24	[29]
	9.85 (c)	733±40	[18]
	9.99 (a)	817±44	[7]
	10.22 (a)	830±44	[7]
	99.20 (b)	674±19	[10]
^{49}Ti	14.50 (a)	931±19	[8]
^{50}Ti	60.80 (a)	853±80	[33]
V	8.80 (a)	730±30	[28]
	9.85 (c)	717^{170}_{120}	[18]
	9.96 (a)	782±62	[7]
	99.90 (b)	692±20	[10]
^{51}V	6.75 (c)	646±43	[27]
	60.80 (a)	787±35	[33]
Cr	28.00 (a)	980±41	[32]
^{52}Cr	60.80 (a)	708±190	[33]
Mn	6.75 (c)	505±43	[27]
^{54}Fe	14.50 (a)	865±16	[8]
	40.00 (a)	856±37	[33]
	60.80 (a)	798±32	[33]
^{56}Fe	14.50 (a)	1012±19	[8]
	28.50 (a)	1140±43	[26]
	40.00 (a)	991±43	[33]
	60.80 (a)	899±32	[33]
^{57}Fe	14.50 (a)	976±14	[8]
	40.00 (a)	1124±130	[33]
	60.80 (a)	783±120	[33]
^{58}Fe	14.50 (a)	1069±20	[8]
	40.00 (a)	1313±130	[33]
	60.80 (a)	1059±90	[33]
Fe	8.90 (a)	680±50	[28]
	9.21 (b)	693±32	[36]
	9.72 (b)	760±31	[36]
	9.85 (c)	865±52	[18]
	9.97 (a)	747±47	[7]
	10.20 (a)	759±47	[7]
	10.23 (b)	809±30	[36]
	10.74 (b)	833±29	[36]
	11.25 (b)	828±29	[36]
	28.00 (a)	973±35	[32]

Continuation

Nucleus	E, MeV	σ_R, mb	Literature
Fe	34.00 (a)	902±72	[3]
	61.00 (a)	617±40	[16]
	99.10 (b)	747±21	[10]
^{59}Co	8.72 (b)	693±36	[36]
	8.80 (a)	825±40	[28]
	9.25 (b)	766±34	[36]
	9.78 (b)	840±31	[36]
	10.32 (b)	902±30	[36]
	28.00 (a)	1068±40	[32]
	28.50 (a)	1169±39	[26]
	40.00 (a)	1042±52	[33]
	60.80 (a)	798±32	[33]
	98.70 (b)	780±22	[10]
^{58}Ni	8.80 (a)	622±55	[28]
	9.14 (b)	547±33	[36]
	14.50 (a)	927±27	[8]
	28.50 (a)	1038±32	[26]
	30.00 (a)	1011±30	[33]
	40.00 (a)	955±34	[33]
	49.50 (a)	856±29	[33]
	60.80 (a)	807±25	[33]
^{60}Ni	8.80 (a)	728±55	[28]
	9.23 (b)	709±37	[36]
	14.50 (a)	978±16	[8]
	28.50 (a)	1053±51	[26]
	40.00 (a)	982±42	[33]
	60.80 (a)	841±30	[33]
^{62}Ni	14.50 (a)	1067±20	[8]
	40.00 (a)	1074±90	[33]
	60.80 (a)	977±76	[33]
^{64}Ni	40.00 (a)	1089±90	[33]
	60.80 (a)	1063±74	[33]
Ni	9.68 (b)	603±33	[36]
	9.85 (c)	713±40	[18]
	9.92 (a)	666±42	[7]
	10.14 (a)	700±42	[7]
	10.20 (b)	659±32	[36]
	10.70 (b)	704±32	[36]
	11.21 (b)	733±30	[36]
	16.33 (a)	898±53	[31]
	28.00 (a)	950±32	[32]
	29.00 (a)	1023±40	[25]
	98.50 (b)	771±22	[10]
^{63}Cu	6.75 (c)	497±41	[27]
	8.70 (a)	746±50	[28]
	9.10 (a)	751±29	[29]
	9.11 (b)	725±35	[36]
	9.85 (c)	845^{92}_{67}	[18]
	10.00 (c)	875±60	[21]
	10.14 (b)	808±30	[36]
	11.18 (b)	855±26	[36]
	14.50 (a)	985±18	[8]
^{65}Cu	6.75 (c)	613±29	[27]
	8.70 (a)	735±55	[28]
	9.10 (a)	754±27	[29]
	9.15 (b)	676±32	[36]
	9.85 (c)	974±76	[18]
	10.00 (c)	855±60	[21]
	10.18 (b)	804±29	[36]
	11.20 (b)	890±26	[36]
	14.50 (a)	1000±14	[8]
Cu	8.78 (b)	680±36	[36]
	8.80 (a)	735±30	[28]
	9.00 (a)	895±80	[24]
	9.05 (a)	768±25	[29]
	9.15 (b)	710±33	[36]
	9.30 (a)	930±70	[6]
	9.52 (b)	740±32	[36]
	9.85 (b)	790±32	[9]
	9.90 (a)	805±43	[7]
	10.12 (a)	816±43	[7]
	10.19 (b)	798±31	[36]
	10.36 (b)	815±30	[36]
	10.70 (b)	830±29	[36]
	10.89 (b)	853±28	[36]
	11.21 (b)	865±28	[36]
	16.37 (a)	955±64	[31]
	28.00 (a)	1024±35	[32]
	98.50 (b)	835±24	[10]
	134.00 (a)	752±68	[89]
^{64}Zn	14.50 (a)	965±16	[8]
^{66}Zn	9.85 (c)	946±85	[18]
	14.50 (a)	1036±19	[8]
^{68}Zn	14.50 (a)	1075±17	[8]
	40.00 (a)	1230±54	[33]
	60.80 (a)	948±38	[33]
Zn	8.75 (a)	726±35	[28]
	8.77 (b)	740±36	[36]
	9.31 (b)	771±33	[36]
	9.83 (b)	810±32	[36]
	9.90 (a)	812±43	[7]
	10.12 (a)	850±43	[7]
	10.36 (b)	844±32	[36]
	10.88 (b)	862±31	[36]
	28.00 (a)	1043±36	[32]
	99.00 (b)	857±24	[10]
Ga	8.80 (a)	825±75	[28]
Ge	28.00 (a)	1105±67	[32]
^{90}Zr	14.50 (a)	902±34	[8]
	30.00 (a)	1249±45	[33]
	40.00 (a)	1316±65	[33]
	49.50 (a)	1214±59	[33]
	60.80 (a)	1144±42	[33]
^{91}Zr	14.50 (a)	929±30	[8]
^{92}Zr	14.50 (a)	1011±23	[8]
^{94}Zr	14.50 (a)	1093±24	[8]
^{96}Zr	60.80 (a)	1241±150	[33]
Zr	9.20 (a)	880±50	[29]
	10.03 (a)	793±83	[7]
	10.25 (a)	800±85	[7]
	99.10 (b)	1077±31	[10]
Nb	9.95 (a)	723±68	[7]
	10.17 (a)	703±68	[7]
	98.80 (b)	1094±31	[10]
Mo	10.03 (a)	721±86	[7]
	98.80 (b)	1119±32	[10]
Rh	10.14 (a)	751±71	[7]
Pd	99.10 (b)	1189±34	[10]
Ag	9.65 (b)	702±67	[36]
	9.90 (a)	718±64	[7]
	10.12 (a)	689±65	[7]
	10.16 (b)	769±60	[36]
	10.67 (b)	788±54	[36]
	11.18 (b)	817±49	[36]
	29.00 (a)	1471±71	[25]
	98.90 (b)	1194±34	[10]
Cd	9.85 (b)	729±72	[36]
	98.80 (b)	1267±36	[10]
	134.00 (a)	1286±103	[89]
In	9.25 (b)	645±85	[36]
	9.76 (b)	694±76	[36]
	10.27 (b)	777±67	[36]
	10.78 (b)	807±60	[36]
	99.30 (b)	1275±36	[10]
^{116}Sn	14.50)a)	1113±45	[8]
	60.80 (a)	1453±60	[33]
^{117}Sn	14.50 (a)	1107±47	[8]
^{118}Sn	14.50 (a)	1194±29	[8]
^{119}Sn	14.50 (a)	1109±50	[8]

Continuation

Nucleus	E, MeV	σ_R, mb	Literature
^{120}Sn	14.50 (a)	1152±34	[8]
	28.50 (a)	1638±68	[26]
	30.00 (a)	1589±50	[33]
	40.00 (a)	1618±73	[33]
	49.50 (a)	1455±72	[33]
Sn	9.99 (a)	610±82	[7]
	10.21 (a)	723±82	[7]
	34.00 (a)	1930±100	[3]
	61.00 (a)	995±70	[16]
	99.10 (b)	1292±37	[10]
Sb	134.00 (a)	1782±143	[89]
La	98.80 (b)	1450±41	[10]
Pr	98.60 (b)	1446±40	[10]
Nd	98.60 (b)	1496±42	[10]
Eu	99.40 (b)	1632±46	[10]
Gd	98.30 (b)	1596±45	[10]
Tb	98.70 (b)	1619±46	[10]
Dy	98.20 (b)	1630±46	[10]
Ho	99.10 (b)	1640±46	[10]
Tm	99.30 (b)	1637±46	[10]
Hf	98.80 (b)	1700±48	[10]
Ta	9.98 (a)	388±195	[7]
	10.20 (a)	331±203	[7]
	98.30 (b)	1710±40	[10]
W	99.30 (b)	1733±49	[10]
Re	99.00 (b)	1730±49	[10]
Pt	99.30 (b)	1815±51	[10]
Au	9.90 (a)	162±104	[7]
	10.08 (b)	150±250	[36]
	10.12 (a)	173±107	[7]
	29.00 (a)	2209±118	[25]
	99.40 (b)	1757±50	[10]
Tl	99.60 (b)	1791±51	[10]
^{208}Pb	28.50 (a)	1865±98	[26]
	30.00 (a)	2117±90	[33]
	40.00 (a)	2023±100	[33]
	49.50 (a)	1842±93	[33]
	60.80 (a)	1993±95	[33]
Pb	9.94 (a)	216±148	[7]
	16.31 (a)	1330±180	[31]
	34.00 (a)	1775±120	[3]
	61.00 (a)	1490±77	[16]
	99.20 (b)	1831±52	[10]
Th	9.98 (a)	49±153	[7]
	99.10 (b)	2006±56	[10]
U	98.90 (b)	2066±57	[10]

Deuteron total reaction cross sections

Nucleus	E, MeV	σ_R, mb	Literature
Be	22.40 (a)	865±21	[39]
B	25.20 (a)	881±30	[40]
C	12.80 (c)	658±86	[42]
	22.40 (a)	896±28	[39]
	25.10 (a)	924±30	[40]
N	1.10	480±80	[52]
Mg	25.30 (a)	1202±55	[40]
^{27}Al	13.35 (b)	1204±27	[43]
	22.40 (a)	1134±35	[39]
	24.90 (a)	1230±55	[40]
Ti	22.40 (a)	1347±66	[39]
	25.30 (a)	1507±38	[40]
V	22.40 (a)	1410±64	[39]
	24.60 (a)	1631±49	[40]
Fe	13.40 (b)	1577±68	[43]
	22.40 (a)	1370±70	[39]
	25.10 (a)	1676±46	[40]
^{59}Co	13.40 (b)	1609±41	[43]
	25.20 (a)	1586±49	[40]
^{58}Ni	10.98 (b)	1375±61	[36]
	12.80 (c)	1589±125	[42]
^{60}Ni	10.06 (b)	1441±60	[36]
	11.10 (b)	1508±63	[36]
	12.80 (c)	1523±120	[42]
	13.59 (b)	1536±125	[43]
^{64}Ni	13.46 (b)	1666±60	[43]
Ni	11.03 (b)	1460±60	[36]
	11.50 (b)	1460±60	[36]
	13.20 (b)	1457±33	[43]
	22.40 (a)	1491±63	[39]
	25.10 (a)	1537±48	[40]
^{63}Cu	10.93 (b)	1482±65	[36]
	13.31 (b)	1609±81	[43]
^{65}Cu	11.00 (b)	1622±80	[36]
	13.42 (b)	1655±63	[43]
Cu	11.01 (b)	1548±66	[36]
	22.40 (a)	1539±61	[39]
	24.90 (a)	1660±49	[40]
Zn	13.43 (b)	1562±46	[43]
	22.40 (a)	1594±65	[39]
	25.30 (a)	1713±50	[40]
Zr	11.80 (a)	1480±200	[52]
	22.40 (a)	1521±106	[39]
	25.10 (a)	1769±71	[40]
Nb	11.80	1400±300	[52]
	22.40 (a)	1666±90	[39]
Rh	22.40 (a)	1747±89	[39]
	25.20 (a)	1848±63	[40]
Ag	13.50 (b)	1644±101	[43]
	22.40 (a)	1635±87	[39]
	25.10 (a)	1855±50	[40]
Sn	13.31 (b)	1979±124	[43]
	22.40 (a)	1563±117	[39]
	25.30 (a)	1786±51	[40]
Ta	22.40 (a)	1637±140	[39]
	25.00 (a)	2034±60	[40]
Au	22.40 (a)	1632±126	[39]
	25.10 (a)	2028±65	[40]
Pb	22.40 (a)	1714±136	[39]
	25.10 (a)	2162±70	[40]
Bi	12.80 (c)	1185±183	[42]
	22.40 (a)	1773±136	[39]
Th	22.40 (a)	1451±165	[39]

Total cross sections of reactions induced by α particles

Nucleus	E, MeV	σ_R, Mb	Literature
Be	40.00 (a)	783±11	[44]
C	15.77 (a)	870±70	[46]
	16.63 (a)	880±70	[46]
	17.49 (a)	780±60	[46]
	18.32 (a)	570±60	[46]
	19.03 (a)	640±60	[46]
	19.55 (a)	690±60	[46]
	20.14 (a)	700±60	[46]
	40.00 (a)	901±16	[44]
^{27}Al	26.40 (b)	1133±25	[43]
	40.00 (a)	1141±21	[44]
Ti	40.00 (a)	1500±37	[44]
V	40.00 (a)	1480±39	[44]
Cr	24.70 (a)	1250±31	[45]
Fe	24.70 (a)	1262±38	[45]
	26.20 (b)	1569±37	[43]
	40.00 (a)	1436±42	[44]
^{59}Co	23.10 (b)	1322±37	[13]
	24.70 (a)	1313±36	[45]
	26.40 (b)	1426±35	[43]
^{60}Ni	26.94 (b)	1550±103	[43]
^{64}Ni	26.40 (b)	1663±57	[43]
Ni	23.20 (b)	1296±53	[13]
	24.70 (a)	1305±53	[45]
	26.40 (b)	1440±52	[43]
	40.00 (a)	1354±37	[44]
^{63}Cu	25.90 (b)	1470±55	[43]
^{65}Cu	26.25 (b)	1546±58	[43]
Cu	23.20 (b)	1350±56	[13]
	24.70 (a)	1393±33	[45]
	25.80 (b)	1495±40	[43]
	40.00 (a)	1646±48	[44]
Zn	24.70 (a)	1383±65	[45]
	26.80 (b)	1691±42	[43]
	40.00 (a)	1639±49	[44]
Zr	40.00 (a)	1771±63	[44]
Nb	23.10 (b)	1346±44	[13]
	27.63 (b)	1470±46	[13]
	40.00 (a)	1728±64	[44]
Mo	40.00 (a)	1782±78	[44]
Pd	23.27 (b)	1260±42	[13]
	27.80 (b)	1433±42	[13]
Ag	23.20 (b)	1292±44	[13]
	27.70 (b)	1443±42	[13]
	40.00 (a)	1846±64	[44]
In	23.20 (b)	1336±46	[13]
	27.80 (b)	1474±44	[13]
Sn	23.25 (b)	1367±47	[13]
	27.80 (b)	1509±45	[13]
	40.00 (a)	1768±78	[44]
Ta	23.25 (b)	647±61	[13]
	27.76 (b)	1068±47	[13]
	40.00 (a)	1886±97	[44]
Pt	23.20 (b)	681±78	[13]
	27.74 (b)	1089±48	[13]
Au	23.10 (b)	580±87	[13]
	27.74 (b)	996±48	[13]
	40.00 (a)	1919±79	[44]
Pb	23.20 (b)	466±86	[13]
	27.90 (b)	801±44	[13]
	40.00 (a)	1892±82	[44]
Bi	23.27 (b)	265±94	[13]
	27.80 (b)	804±44	[13]
	40.00 (a)	1853±105	[44]
Th	40.00 (a)	1761±105	[44]

Total cross sections of reactions induced by ^{3}He particles

Nucleus	E, MeV	σ_R, Mb	Literature
Mg	28.50 (a)	1235±25	[47]
Al	28.90 (a)	1328±17	[47]
Fe	28.10 (a)	1570±45	[47]
Ni	28.70 (a)	1695±30	[47]
Cu	28.70 (a)	1775±39	[47]
Ag	28.70 (a)	2020±60	[47]

Note: a) attenuation method using the coincidence-anticoincidence technique (CA); b) attenuation method using two Faraday cups as detectors (FC); c) summation method; d) method of recoil nuclei.

[1]M. L. Goldberger and K. M. Watson, Collision Theory, New York (1954).
[2]J. T. Holdeman and R. M. Thaler, Phys. Rev. B **139**, 1186 (1965).
[3]T. J. Gooding, Nucl. Phys. **12**, 241 (1959).
[4]E. J. Burge, Nucl. Phys. **13**, 511 (1959).
[5]R. A. Giles and E. J. Burge, Rev. Scient. Instrum. **34**, 709 (1963).
[6]G. W. Greenlees and O. N. Jarvis, Proc. Phys. Soc. **78**, 1275 (1961).
[7]B. D. Wilkins and G. Igo, Phys. Rev. **129**, 2198 (1963).
[8]J. F. Dicello, G. Igo, and M. L. Roush, Phys. Rev. **157**, 1001 (1967).
[9]K. Bearpark, W. R. Graham, and W. R. Jones, Nucl. Instrum. and Methods **35**, 235 (1965).
[10]P. Kirkby and W. T. Link, Canad. J. Phys. **44**, 1847 (1966).
[11]L. V. Dubar' *et al.*, Prib. Tekh. Éksp., No. 3, 36 (1972).
[12]L. I. Slyusarenko and V. V. Tokarsvskii, Prib. Tekh. Éksp., No. 4, 24 (1972).
[13]W. Karcz *et al.*, Acta Phys. Polonica B **5**, 115 (1974).

[14]M. A. Melkanoff *et al.*, Phys. Rev. **106**, 793 (1967).
[15]A. E. Glassgold and P. J. Kellogg, Phys. Rev. **107**, 1372 (1957); Phys. Rev. **109**, 1291 (1958).
[16]V. Meyer, R. M. Eisberg, and R. F. Carlson, Phys. Rev. **117**, 1334 (1960).
[17]R. G. P. Voss and R. Wilson, Proc. Roy. Soc A **236**, 41 (1956).
[18]V. Meyer and N. M. Hintz, Phys. Rev. Lett. **5**, 207 (1960).
[19]A. E. Glassgold *et al.*, Phys. Rev. **106**, 1207 (1957).
[20]J. S. Nodvik and D. S. Saxon, Phys. Rev. **117**, 1539 (1960).
[21]R. D. Albert and L. F. Hansen, Phys. Rev. Lett. **6**, 13 (1961).
[22]F. Bjorklund and S. Fernbach, Phys. Rev. **109**, 1295 (1958).
[23]B. R. Easlea, Proc. Phys. Soc. **78**, 1285 (1961).
[24]R. F. Carlson *et al.*, Nucl. Phys. **36**, 511 (1962).
[25]M. Q. Makino, C. N. Waddell, and R. M. Eisberg, Nucl. Phys. **50**, 145 (1964).
[26]B. W. Ridley and J. F. Turner, Nucl. Phys. **58**, 497 (1964).
[27]G. F. Dell, W. D. Ploughe, and H. J. Hausman, Nucl. Phys. **64**, 513 (1965).
[28]P. J. Bulman, G. W. Greenlees, and M. J. Sametband, Nucl. Phys. **69**, 536 (1965).
[29]P. J. Bulman and J. A. R. Griffith, Nucl. Phys. A **111**, 315 (1968).
[30]F. G. Perey, Phys. Rev. **131**, 745 (1963).
[31]R. E. Pollock and G. Schrank, Phys. Rev. B **140**, 575 (1965).
[32]M. Q. Makino *et al.*, Phys. Lett. **9**, 178 (1964).
[33]J. J. H. Menet *et al.*, Phys. Rev. C **4**, 1114 (1971).
[34]J. Delaunay, B. Delaunay, and J. P. Passerieux, In: Comp. Rend. Congr. Internat. Phys. Nucl., Vol. 2, Paris (1964), p. 880.
[35]K. Bearpark, W. R. Graham, and G. Jones, In: Compt. Rend. Congr. Intern. Phys. Nucl. Vol. 2, Paris (1964), p. 864.
[36]K. Bearpark, W. R. Graham, and G. Jones, Nucl. Phys. **73**, 206 (1965).
[37]J. F. Dicello and G. Igo, Phys. Rev. C **2**, 488 (1970).
[38]D. G. Montague *et al.*, Nucl. Phys. A **199**, 457 (1973).
[39]B. Wilkins and G. Igo, Phys. Lett. **3**, 48 (1962).
[40]S. Mayo *et al.*, Nucl. Phys. **62**, 393 (1965).
[41]H. R. E. Tjin, A. Djie, and K. W. Brockman, Nucl. Phys. **74**, 417 (1965).
[42]A. Budzanowski *et al.*, Nucl. Phys. **49**, 144 (1963).
[43]L. V. Dubar' *et al.*, In: Programma i Tezisy Dobladov XXII Ezhegodnogo Soveshchaniya po Yadernoĭ Spektroskopii i Strukture Atomnogo Yadra (Program and Abtracts of Papers at 22nd Annual Conference on Nuclear Spectroscopy and Nuclear Structure), Part II, Nauka, Moscow (1972), p. 68.
[44]G. Igo and B. D. Wilkins, Phys. Rev. **131**, 1251 (1963).
[45]A. Budzanowski *et al.*, Nucl. Phys. A **106**, 21 (1968).
[46]E. Labie *et al.*, Nucl. Phys. A **205**, 81 (1973).
[47]R. Balcarcel and J. A. R. Griffith, Phys. Lett. B **26**. 213 (1968).
[48]D. J. Baugh *et al.*, Nucl. Phys. A **95**, 115 (1967).
[49]P. E. Hodgson, Nucl. Phys. **21**, 28 (1960).
[50]D. J. Baugh, Nucl. Phys. A **131**, 417 (1969).
[51]F. D. Becchetti and G. W. Greenlees, Phys. Rev. **182**, 1190 (1969).
[52]P. E. Hodgson, Adv. Phys. **15**, 329 (1966).
[53]M. P. Fricke *et al.*, Phys. Rev. **156**, 1207 (1967).
[54]C. B. Fulmer *et al.*, Phys. Rev. **181**, 1565 (1969).
[55]C. M. Perey and F. G. Perey, Phys. Rev. **132**, 755 (1963).
[56]L. V. Dubar' *et al.*, Izv. Akad. Nauk SSSR, Ser. Fiz. **38**, 2186 (1974).
[57]J. R. Huizenga and G. Igo, Nucl. Phys. **29**, 462 (1962).
[58]G. Igo, Phys. Rev. **115**, 1665 (1959).
[59]H. W. Bertini, Phys. Rev. C **5**, 2118 (1972).
[60]A. P. Klyucharev and N. Ya. Rutkevich, Zh. Éksp. Teor. Fiz. **38**, 285 (1960); [Sov. Phys.-JETP **11**, 207 (1960)]; N. Ya. Rutkevich *et al.*, Dokl. Akad. Nauk SSSR **130**, 1008 (1960) [Sov. Phys.-Doklady **5**, 118 (1960)].
[61]O. F. Nemets *et al.*, Yad. Fiz. **4**, 293 (1966) [Sov. J. Nucl. Phys. **4**, 212 (1967)].
[62]V. P. Bochin *et al.*, Zh. Éksp. Teor. Fiz. **47**, 855 (1964) [Sov. Phys.-JETP **20**, 570 (1965)].
[63]J. J. Lucas and J. Menet, Rapport Annuel, 1971, Université scientifique et médicale de Grenoble, p. 60.
[64]L. V. Dubar' *et al.*, Yad. Fiz. **20**, 624 (1974) [Sov. J. Nucl. Phys. **20**, 335 (1975)].
[65]L. R. B. Elton, Nucl. Phys. **23**, 681 (1961).
[66]Yu. A. Berezhnoi, Ukr. Fiz. Zh. **6**, 275 (1961).
[67]R. F. Frosch *et al.*, Phys. Rev. **174**, 1380 (1968).
[68]V. M. Khvastunov *et al.*, Yad. Fiz. **10**, 217 (1969) [Sov. J. Nucl. Phys. **10**, 122 (1970)].
[69]V. M. Khvastunov *et al.*, Nucl. Phys. A **146**, 15 (1970).
[70]L. R. B. Elton, Nuclear Sizes, London (1971).
[71]A. N. Vereshchagin *et al.*, Uprugoe Rasseyanie Deĭtronov s Énergieĭ 13.6 MeV Yadrami (Elastic Scattering of 13.6-MeV Deuterons on Nuclei), Kiev, Institute of Physics, Academy of Sciences of the Ukrainian SSR (1970).
[72]A. S. Litvinenko *et al.*, Yad. Fiz. **15**, 1104 (1972) [Sov. J. Nucl. Phys. **15**, 611 (1972)].
[73]O. F. Nemets *et al.*, Ukr. Fiz. Zh. **16**, 403 (1971).
[74]I. E. Kashuba and V. P. Kozin, Ukr. Fiz. Zh. **13**, 51 (1968).
[75]A. Akhieser and I. Pomeranchuk, J. Phys. (USSR) **9**, 471 (1945).
[76]R. H. Venter and W. E. Frahn, Ann. Phys. (N. Y.) **27**, 401 (1964).
[77]W. E. Frahn, In: Fundamentals in Nucl. Phys. IAEA, Vienna (1967), p. 3.
[78]E. V. Inopin, Zh. Éksp. Teor. Fiz. **48**, 1620 (1965) [Sov. Phys.-JETP **21**, 1090 (1965)].
[79]B. I. Tishchenko and A. V. Shebeko, Zh. Éksp. Teor. Fiz. **50**, 1674 (1966) [Sov. Phys.-JETP **23**, 1113 (1966)].
[80]V. I. Tishchenko and Yu. P. Mel'nik, Yad. Fiz. **5**, 1012 (1967) [Sov. J. Nucl. Phys. **5**, 722 (1967)].
[81]V. I. Tishchenko and E. V. Inopin, Yad. Fiz. **7**, 1029 (1968) [Sov. J. Nucl. Phys. **7**, 618 (1968)].
[82]V. S. Bulkin and V. V. Tokarevskiĭ, Yad. Fiz. **19**, 1239 (1974) [Sov. J. Nucl. Phys. **19**, 634 (1974)].
[83]V. Yu. Gonchar and K. S. Zheltonog, Yad. Fiz. **13**, 84 (1971) [Sov. J. Nucl. Phys. **13**, 48 (1971)].
[84]G. R. Satchler, Nucl. Phys. A **91**, 75 (1967).
[85]G. R. Satchler, In: Isospin in Nucl. Phys. (ed. D. H. Wilkinson), North Holland (1969), p. 389.
[86]I. N. Simonov, K. O. Terenetskiĭ, and V. V. Tokarevskiĭ, Izv. Akad. Nauk SSSR, Ser. Fiz. **34**, 1748 (1970) [Bull. Acad. Sci. USSR, Phys. Ser.].
[87]M. Q. Makino, C. N. Waddell, and R. M. Eisberg, Nucl. Phys. **68**, 378 (1965).
[88]R. A. Giles and E. J. Burge, Nucl. Phys. **50**, 327 (1964).
[89]J. M. Cassels and J. D. Lawson, Proc. Phys. Soc. **67**, 125 (1954).
[90]C. Bergman and R. K. Hobbie, Phys. Rev. C **3**, 1729 (1971).
[91]M. Takeda, S. Kato, and T. Yamazaki, J. Phys. Soc. Japan, **30**, 56 (1971).
[92]M. Takeda, S. Kato, and T. Yamazaki, J. Phys. Soc. Japan, **31**, 625 (1971).
[93]A. M. Lane, Nucl. Phys. **35**, 676 (1962).

Translated by Julian B. Barbour